Earthquake Locations Determined by the Southern Alaska Seismograph Network for October 1971 through May 1989

By Kent A. Fogleman, John C. Lahr, Christopher D. Stephens and Robert A. Page

Open-File Report 93-309, v. 1.1

U.S. Department of the Interior
U.S. Geological Survey

U.S. Department of the Interior
KEN SALAZAR, Secretary

U.S. Geological Survey
Marcia K. McNutt, Director

U.S. Geological Survey, Reston, Virginia: 1993
Revised 2012

Suggested citation:
Fogleman, K.A., Lahr, J.C., Stephens, C.D., and Page, R.A., 1993, revised 2012, Earthquake locations determined by the southern Alaska seismograph network for October 1971 through May 1989: U.S. Geological Survey Open-File Report 93-309, Version 1.1, 54 p. and data files, available at *http://pubs.usgs.gov/of/1993/0309/*.

Contents

Figures

Tables

Appendixes

Earthquake Locations Determined by the Southern Alaska Seismograph Network for October 1971 through May 1989

By Kent A. Fogleman[1], John C. Lahr[2], Christopher D. Stephens[1,] and Robert A. Page[3]

[1]U.S. Geological Survey, Earthquake Science Center (ESC), Menlo Park, Calif.
[2] U.S. Geological Survey, Geophysicist deceased
[3] U.S. Geological Survey, Geophysicist emeritus, ESC, Menlo Park, Calif.

Introduction

The U.S. Geological Survey (USGS) operated a regional network of seismographs in southern Alaska from 1971 to the mid 1990's. The principal purpose of this network was to record seismic data to be used to precisely locate earthquakes in the seismic zones of southern Alaska, delineate seismically active faults, assess seismic risks, document potential premonitory earthquake phenomena, investigate current tectonic deformation, and study the structure and physical properties of the crust and upper mantle. A task fundamental to all of these goals was the routine cataloging of parameters for earthquakes located within and adjacent to the seismograph network.

The initial network of 10 stations, 7 around Cook Inlet and 3 near Valdez, was installed in 1971. In subsequent summers additions or modifications to the network were made. By the fall of 1973, 26 stations extended from western Cook Inlet to eastern Prince William Sound, and 4 stations were located to the east between Cordova and Yakutat. A year later 20 additional stations were installed. Thirteen of these were placed along the eastern Gulf of Alaska with support from the National Oceanic and Atmospheric Administration (NOAA) under the Outer Continental Shelf Environmental Assessment Program to investigate the seismicity of the outer continental shelf, a region of interest for oil exploration. Since then the region covered by the network remained relatively fixed while efforts were made to make the stations more reliable through improved electronic instrumentation and strengthened antenna systems. The majority of the stations installed since 1980 were operated only temporarily (from one to several years) for special studies in various areas within the network. Due to reduced funding, the network was trimmed substantially in the summer of 1985 with the closure of 15 stations, 13 of which were located in and around the Yakataga seismic gap. To further reduce costs, two telephone circuits were dropped and multiple radio relays were installed in their place. This economy reduced the reliability of these telemetry links. In addition, data collection from the areas around Cordova and Yakutat was compromised by

the necessity of relying on triggered event recording using PC-based systems (Rogers, 1993) that were not fully developed and which proved to be less reliable than anticipated.

The principal means of recording throughout the time period of this catalog was 20-channel oscillographs on 16-mm film (Teledyne Geotech Develocorder, Model RF400 and 4000D). Initially one Develocorder was operated at the USGS Alaskan headquarters in Anchorage, but in 1972 recording was shifted to the National Oceanic and Atmospheric Administration (NOAA) Palmer Observatory (currently the West Coast and Alaska Tsunami Warning Center). The Develocorders were turned off at the end of May 1989, and after that time recording was done in digital format at the Geophysical Institute of the University of Alaska in Fairbanks (GIUA). Thus, this catalog covers the entire period of film recording.

Instrumentation

The locations of seismograph stations of the USGS network that contributed to this catalog are shown in Figure 1 along with stations operated by other institutions from which readings were obtained. Station coordinates and operational dates are listed in Table 1. Most of the USGS stations had only single, vertical-component sensors, but horizontal components seismometers were also operated at a few selected sites (marked by asterisks in Table 1).

The instrumentation used in the USGS seismograph network is illustrated in the block diagram in Figure 2. The standard equipment at each field site included: a vertical seismometer with a natural frequency of 1.0 Hz (Mark Products, Model L-4C); an electronics package consisting of an amplifier, voltage-controlled oscillator (Develco Model 6203 or equivalent) until about 1980, and then an A1VCO with calibrator and gain-ranging (Rogers and others, 1980); and either "air-cell" storage batteries, or a solar panel with 80 amp-hr storage batteries.

Data were telemetered via a combination of VHF (162-174 MHz) radio links and leased telephone circuits, some of which used satellite links having a 0.27 s transmission delay per hop. The radio equipment consisted of low-power (100 mW) transmitters and receivers, many adapted from HT-200 Motorola handie-talkie transceivers, and either Yagi antennae with 9 db directional gain (Scala, Model CAS-150) or log-periodic antennae (Scala, Model CL-150). At the receive sites, where the seismic signals entered the telephone circuits, base-station radio receivers (G.E. Model R46AP66B) with greater sensitivity were used. The central recording facility incorporated a bank of discriminators (USGS designed NCER J101 or Develco Model 6203), four 16 mm-film 20-channel oscillographs (Teledyne Geotech Develocorder, Model RF400 and 4000D), a 14-track FM magnetic tape recorder (Bell and Howell Model VR3700B), three 3-channel drum recorders (Teledyne Geotech Helicorder, Model RV301B), and a time-code generator (Datum, Model 9100).

The principle of operation was as follows: the seismometer translated ground velocity into an electrical voltage that was fed into the amplifier/VCO unit. There the amplified voltage caused the frequency of VCO to fluctuate about its center frequency. The frequency-modulated (FM) tone from the amplifier/VCO unit was carried directly to the recording site by VHF radio links and/or voice-grade telephone circuits. Signals from eight seismograph stations could be transmitted on a single telemetry circuit using standard frequency division multiplexing techniques with a 340 Hz

separation between carriers and a constant bandwidth of 250 Hz per channel. The channel center frequencies ranged from 680 to 3,060 Hz. A ninth channel with center frequency of 340 Hz and 125 Hz bandwidth was also commonly used. At the recording site the FM seismic signal was demodulated by a discriminator. The demodulated signal, which was simply an amplified and filtered form of the initial signal from the seismometer, was recorded on the oscillograph and tape recorder together with time signals from the time-code generator. Twenty-four hours of data from 18 stations could be recorded on a single 43 m-long roll of 16-mm film, while data from nine stations could be recorded on a single track of a 2,195 m-long, 14-track tape. A number of stations were also recorded on Helicorder records for monitoring purposes.

Figure 3 illustrates the response characteristics of the entire seismic system from seismometer to film viewer. The response level at each station was adjusted in steps of 6 decibels so that the ambient seismic noise produced a small deflection of the trace on the film. As a result, the actual response for an individual station may differ from that of the typical station by a factor of 2, 4, 8, etc. The magnification of the typical station was about 6×10^4 at 1 Hz and 1×10^6 at 10 Hz.

Digital seismic-event recorders were developed internally and deployed to temporarily augment network recording in areas of interest. A description of these instruments can be found in Rogers and Lahr (1986) and Fogleman and Rogers (1987).

Data Processing

The 16-mm films, magnetic tapes, and Helicorder records were mailed weekly from the Alaska Tsunami Warning Center in Palmer, Alaska to the USGS in Menlo Park, California where the seismic data were processed by the following multi-step routine:

1. Scanning. The scan film, which recorded data from 18 stations distributed throughout the network, was scanned to identify all seismic events, including those of local, regional, and teleseismic origin, and to note the earliest P-arrival time, the time interval between the P and S phases (S-P time), and the duration of the signal (F-P coda time) for the first 3 stations. Stations not recorded on the scan film were arranged on the remaining films by geographic region.

2. Timing. For the "well-recorded" local earthquakes identified in the scanning process, the following data were read from each station: P- and S-wave arrival times, direction of first motion, duration of signal in excess of a given threshold amplitude, and period and peak-to-trough amplitude of maximum recorded signal. The P and S times were assigned weights according to the reader's confidence of the precision of the picks. The precision was influenced by the impulsiveness of the phases and the recording quality. Weights range from a full weight (coded 0) for the highest quality readings to no weight (coded 4) for times too poor to be used for hypocenter determination.

From October 1971 through the end of September 1973, the criteria for choosing earthquakes to be timed were based on S-P times and the number of stations that clearly record the earthquake. Beginning with October 1973, an additional criterion based on the signal duration was

used. The area within which earthquake locations were routinely determined changed a number of times since 1971. The various criteria from October 1971 to May 1989 used to determine which earthquakes to time are summarized in Appendix C. From September 1, 1985 to May 31, 1989, for example, the area was bounded approximately by longitudes 156° and 138°W and by latitudes 58° and 62.5°N, and was subdivided into western and eastern regions at longitude 145°W. In the western region, only events with average signal durations longer than 30s were routinely timed. In the eastern region, all earthquakes that were recorded by at least three stations and that produce at least four clear arrivals were timed. These criteria were established to select from the large number of earthquakes recorded by the network those shocks that were of greatest interest to current research objectives. In areas where special studies were being conducted, exceptions to the standard criteria were often made in order to locate more events.

Until October 1982 all of the available data recorded on the Develocorder films were read for each timeable earthquake. Since then, in order to keep the data processing current, only the scan film and the film(s) which contain the stations in the region in which the earthquake occurred were timed. A record of which films were timed for each earthquake was kept with the daily scan sheet.

Due to changes in the distribution of stations, to variations in seismicity rates, and to modifications in the criteria used for selecting which events to locate, the number of shocks located each month varied with time (Figure 4). The large increase seen beginning with March 1979 was due mainly to the aftershock sequence of the February 1979, M_S 7.1 St. Elias earthquake which elevated the level of activity until the mid 1980's. The gradual decay in the number of events per month from 1979 to 1988 was due partially to decay in the rate of St. Elias aftershocks and to the closure of 15 stations, 13 of which were located in and around the Yakataga seismic gap, in the summer of 1985. Large spikes in the monthly number between 1982 and 1988 were due mainly to aftershock sequences. The large increase beginning in 1989 was due predominantly to the integration of data processed by the Geophysical Institute of the University of Alaska in Fairbanks with the USGS southern Alaska data.

The bulk of the timing was done by projecting the seismic traces from the film onto a one-film wire-grid or four-film sonic (Astrue and others, 1983) computer-based digitizing table, where the P- and S-phases, maximum amplitude, and coda duration were input as x-y coordinates into a computer and reformatted for input into a hypocentral location program. Since the fall of 1983, some of the timing utilized digital waveform data obtained by digitizing the daily FM magnetic tapes at 100 samples per second. In the latter case an interactive, computer-based processing system (Stevenson, 1978) was used to display the waveforms and to pick the phase data. Starting in July 1988, the Geophysical Institute of the University of Alaska (GIUA), Fairbanks began recording 13 USGS stations along with those in its own network as digital waveform files. All events that triggered the GIUA automatic detection and recording system were located regardless of magnitude or location. Consequently, shocks within the USGS routine processing borders that would normally not have been processed by the USGS were also located. The digital data were timed using the program XPICK (Robinson, 1990). Duplicate readings by GIUA staff for earthquakes processed by the USGS were typically weighted out.

3. Initial computer processing. The phase data for the timed events were batch processed by computer using the program HYPOELLIPSE (Lahr, 1989, 1999) to obtain origin times, hypocenters, magnitudes and, if desired, first-motion plots for fault-plane solutions. The HYPOELLIPSE computer program determines hypocenters by minimizing differences between observed and computed traveltimes through an iterative least-squares scheme. In many respects the program is similar to HYPO71 (Lee and Lahr, 1972), from which it was derived. Important features available in HYPOELLIPSE, but not in HYPO71, include multiple velocity and delay models, calculation of confidence ellipsoids, and incorporation of a station-history data base to keep the station gains and polarities updated.

The earthquake locations are based on P- and S-arrivals. S-arrivals provide important constraints on epicenters of shocks outside the network, and depths of events in the Wadati-Benioff zones beneath Cook Inlet and the Wrangell volcanoes (see section on Focal Depths). For some large events timed from the films, S-arrivals could not be read at any station because the traces on the film overlapped each other or were too faint to read. However, S-arrivals not readable from the films were often picked on paper records generated from playbacks of the magnetic tapes.

4. Analysis of initial computer results. Each hypocentral solution was checked for: large traveltime residuals (see section on Analysis of Hypocentral Quality), a root-mean-square (RMS) residual greater than 1 s, a focal depth greater than 35 km in an area where no Wadati-Benioff zone was known to exist, individual station magnitudes which differed from the average event magnitude by more than 0.5, and a poor spatial distribution of stations. Events with potential timing errors were re-read and additional readings, including those from sources other than the USGS network, were sought for shocks with a poor distribution of recording stations.

Initially, when the network spanned a relatively small area , traveltime residuals greater than 0.4 s were checked for data that was cataloged. As the network expanded eastward, it became necessary to increase the threshold for checking traveltime residuals due to the increase in the average epicentral distance to the stations used to locate the earthquakes. Beginning with 1978 data, the criterion for checking traveltime residuals was to check: the five closest stations for P-residuals greater than 0.6 s and S-residuals greater than 1.0 s; the stations beyond the first five and up to 150 km from the epicenter for P- and S-residuals greater than 0.9 s and 1.5 s, respectively; and stations with an epicentral distance between 150 to 350 km for P-residuals greater than 1.5 s and S-residuals greater than 2.0 s. Arrivals at stations with epicentral distances greater than 350 km were generally weighted out by HYPOELLIPSE and checked for P- and S-residuals greater than 2.0 s and 3.0 s, respectively.

5. Final computer processing. Poor hypocentral solutions were rerun with corrected and/or additional data, and the new solutions were checked for large residuals that might indicate remaining errors. Corrections were made as required before the final computer run. Generally no more than three computer runs were allowed for any earthquake by an analyst. Additional runs were made by a geophysicist to correct problem events. An empirical study of 100 earthquakes from October and November 1979 revealed that correcting all large traveltime residuals for each solution regardless of the overall quality of the solution resulted in little improvement in hypocenter precision and was time consuming. The high-quality solutions with only a few large traveltime

residuals generally changed less than one minute in latitude and longitude and one km in depth with additional re-reads and computer runs. Consequently, since January 1980, earthquakes with only a few large traveltime residuals were checked only if the analyst felt the hypocentral solution might be affected.

Velocity Models

Our experience with locating earthquakes in southern Alaska suggest that significant lateral variations are present in the velocity structure across the network. Such variations might be expected from the complex geology and tectonics of the region (e.g., Plafker, 1967; Page and others, 1986). Over the years different methods have been used to account for variations in the crustal structure across southern Alaska. There have also been changes in the location program HYPOELLIPSE which would modify the computed locations (Lahr, 1989, 1999). For these reasons, all of the earthquake data from October 1971 through May 1989 were relocated using a single set of control parameters. Three velocity models were used in locating the earthquakes (Table 2). The Southern Alaska Model was based on a study of earthquakes below the Kenai Peninsula (Model A, Matumoto and Page, 1969); the Northern Alaska Model was developed by the Geophysical Institute of the University of Alaska, Fairbanks (N. Biswas, personal communication, 1988); the Gulf of Alaska Model was based on a study of the 1987 and 1988, M_w 7.9 and M_w 7.8, Gulf of Alaska earthquakes (Lahr and others, 1988a) and their aftershocks.

It is recognized that a model comprised of uniform horizontal layers is a poor representation of the actual velocity structure in the vicinity of a subduction zone (Mitronovas and Isacks, 1971; Jacob, 1972, McLaren and Frohlich, 1985); however, such a model does have the advantage of simplifying the computation of traveltimes. In order to determine any bias that might result from the approximation, a set of events in the Wadati-Benioff zone below Cook Inlet was relocated using a ray-tracing program of E. R. Engdahl and incorporating a more realistic, three-dimensional velocity model (Lahr and others, 1974; Lahr, 1975). Hypocenter shifts due to the oversimplified flat-layer model ranged from near zero at a depth of 60 km to as great as 25 km at 160-km depth. The offsets were oriented in such a way that the dip of the Wadati-Benioff zone would appear to be too great for locations based on a flat-layered model.

The choice of which velocity model to use in calculating the traveltime from an earthquake to a given station was based on the location of the earthquake. Table 3 summarizes the assignment of starting depth, velocity model, and station delay models.

Traveltime Delay Models and Trial Focal Depths

Corrections for P-phase and S-phase traveltime delays were applied at stations in the network that have consistently large residuals for most earthquakes (Table 4). The particular correction that was used to locate an earthquake was determined by the region in which the earthquake occurs (see Table 3).

Additional corrections were applied at several stations to correct for telemetry delays associated with one or more satellite hops (0.27 s transmission delay per hop) used in the telephone relay of the signal and were kept updated in the station-history data base.

Because the depths of earthquakes in southern Alaska range from the surface to almost 200 km, hypocenters were computed starting at several trial focal depths to find the best solution. First, fixed-depth solutions were computed at depths z = 0 and 75 km, and a free-depth solution starting at z = 75 km was determined. If the latter solution had z < 20 km and a significantly lower RMS than at z = 0, then it was taken as the final solution. If, on the other hand, the z = 0 depth had a significantly lower RMS, then a free-depth solution starting at z = 0 was used as the final solution. If neither the free-depth solution starting at 75 km nor the fixed-depth solution had significantly lower RMS, then the solution with the lower RMS was considered the best. Alternatively, if the free-depth solution starting at 75-km depth has z greater than or equal 20 km, then a solution with z fixed at 7.5 km was computed. Of the two fixed-depth solutions at 0 and 7.5 km, the one with lower RMS was used as a starting location for a free-depth solution. If the latter solution was within 7.5 km of the free solution that started at 75 km, then the solution with the lower RMS was reported as final. If the solutions were more than 5 km apart, then the one with lower RMS was reported as final. In the Gulf of Alaska where the velocity structure was poorly understood and hypocenters were not well constrained all of the depths were fixed at 10 km (see Table 3 for the border that was used to define the Gulf of Alaska).

Magnitudes

Magnitudes are determined from either the coda duration or the maximum trace amplitude. Eaton and others (1970) approximated the local Richter magnitude, the definition of which is tied to maximum trace amplitudes recorded on standard Wood-Anderson horizontal torsion seismographs, by magnitude based on maximum trace amplitudes recorded on high-gain, high-frequency vertical seismographs, such as those operated in the Alaskan network. The amplitude magnitude, XMAG or M_X, used in this catalog is based on the work of Eaton and his co-workers and is given by the expression (Lee and Lahr, 1972):

$$XMAG = \log_{10} A - B_1 + B_2 \log_{10} D^2 \qquad (1)$$

where A is the equivalent maximum trace amplitude in millimeters on a standard Wood-Anderson seismograph, D is the hypocentral distance in kilometers, and B_1 and B_2 are constants. Differences in the frequency response of the two seismograph systems are accounted for in A. It is assumed, however, that there is no systematic difference between the maximum horizontal ground motion and the maximum vertical motion. The term $-B_1 + B_2 \log_{10} D^2$ approximates Richter's $-\log_{10}A_o$ attenuation function (Richter, 1958, p. 342), where A_o is the trace amplitude for an earthquake of magnitude zero as a function of epicentral distance as observed for earthquakes in southern California. The constants used are $B_1 = 0.15$ and $B_2 = 0.08$ for D= 1-200 km, and $B_1 = 3.38$ and $B_2 = 1.50$ for D = 200-600 km. These constants have not been calibrated for southern coastal Alaska.

Coda durations are also used for determining magnitude because the maximum trace amplitude is often off scale due to the limited dynamic range of the film recording. For small, shallow earthquakes in central California, Lee and others (1972) express the duration magnitude, FMAG or M_D at a given station by the relation:

$$FMAG = -0.87 + 2.00 \log_{10} T + 0.0035 d \qquad (2)$$

where T is the signal duration in seconds from the P-wave onset to the point on the Develocorder film where the peak-to-peak trace amplitude of the coda envelope measured on a film viewer with 20X magnification falls below 1 cm (F time), and d is the epicentral distance in kilometers.

Comparison of XMAG and FMAG estimates from equations (1) and (2) for 77 southern Alaskan shocks in the depth range 0 to 150 km and in the magnitude range 1.5 to 3.5 reveals a systematic linear decrease of FMAG relative to XMAG with increasing focal depth. However, no systematic dependence of T on D has been found. The following equation, including a linear depth-dependence term but not a distance term, is therefore used for Alaska:

$$FMAG = -1.15 + 2.00 \log_{10} T + 0.007 Z \qquad (3)$$

where Z is the focal depth in kilometers.

The coda duration magnitudes calculated from the network data are systematically less than the magnitudes reported in the Earthquake Data File (EDF) of NOAA (Lahr and Stephens, 1983). Based on a preliminary analysis (John Lahr, unpublished data), the empirical relationship between body-wave magnitude m_b and duration magnitude, M_D is:

$$m_b = 1.4 M_D - 0.39 \qquad (4)$$

The magnitude preferentially assigned to each earthquake in this catalog is the mean of the FMAG (equation 3) estimates obtained for USGS stations. When no FMAG can be determined, the mean of the XMAG (equation 1) estimates for USGS stations is reported. For some earthquakes no XMAG or FMAG estimates are available and a magnitude calculated by another organization is used when available. Earthquakes with published magnitudes such as mb, Ms, or Mw greater than 5 were preferentially used instead of FMAG when no XMAG was available.

Analysis of Hypocentral Quality

Two types of errors enter into the determination of hypocenters: systematic errors limiting the accuracy and random errors limiting the precision. Systematic errors result mainly from incorrect modeling of the seismic velocity structure in the earth and from incorrect phase identification. Random errors arise primarily from timing errors; their effect on the solution for each earthquake can be estimated through the use of standard statistical techniques.

The HYPOELLIPSE computer program determines hypocenters by minimizing differences between observed and computed traveltimes through an iterative least-squares process. For each earthquake, HYPOELLIPSE calculates the lengths and orientations of the principal axes of the joint confidence ellipsoid. The one-standard-deviation confidence ellipsoid describes the region of space within which one is 68 percent confident that the hypocenter lies, assuming that the only source of error is random reading errors. The confidence ellipsoid is a function of the geometry of the stations recording a particular event, the velocity model assumed, and the standard error of the arrival times; it is a measure of the precision of the hypocentral solution (see Figure 10). Repeated readings of the same phases by four seismologists have established that the standard deviation is as small as 0.01 to 0.02 s for the most impulsive arrivals and as large as 0.10 to 0.20s for emergent arrivals. The confidence ellipsoids are computed for a standard deviation of 0.1 s and therefore likely overestimate the 68 percent confidence regions. The standard deviation of the residuals for an individual solution is not used to calculate the confidence ellipsoid because it contains information not only about random reading errors but also about the incompatibility of the velocity model to the data.

In a few extreme cases the value calculated for one of the ellipsoid axes becomes very large corresponding to a spatial direction with very great uncertainty. In these cases an upperbound length of 50 km is tabulated. In most hypocentral solutions, the epicentral precision (SEH) is better determined than the focal depth precision (SEZ) so that SEH is generally smaller than SEZ.

To fully evaluate the quality of a hypocenter one must consider both the size and orientation of the confidence ellipsoid and the root-mean-square (RMS) residual (see description of RMS in Section 2.3.4 in HYPOELLIPSE manuel). In addition to reflecting random errors, the RMS residual can be large due to the misfit of the velocity model to the actual velocities within the earth, misinterpretation of phases, and systematic timing errors. In areas where the velocity structure is accurately known, a large RMS residual would probably indicate errors in the phase data. If the assumed velocity model does not represent the true seismic velocity structure within the earth, the RMS residuals could be large and reflect the incompatibility; alternatively, the RMS residuals could be small and not indicate the actual error in a mislocated hypocenter.

Other parameters provided by HYPOELLIPSE that are helpful in evaluating the quality of a hypocentral solution are: 1) GAP, the largest azimuthal separation between stations measured in degrees at the epicenter. If GAP exceeds 180°, the earthquake lies outside the network of stations used to locate the shock, and the solution is generally less reliable than that for an event occurring inside the network. 2) D1, the epicentral distance in kilometers of the closest station used in the solution. Solutions where the calculated depth is greater than D1 generally have smaller SEZ values (better depth precision) than events that have calculated depths less than the epicentral distance to the closest station. 3) NP and NS, the number of P- and S-arrivals, respectively, used in the solution. The accuracy of the solutions generally improves with an increase in the number of P- and S-arrivals. The RMS residual may actually increase, however, if distant stations are included in locating an event, because the differences between the observed and calculated traveltimes commonly increase with increasing epicentral distance due to the errors in the assumed velocity model.

Hypocenter Precision

The precision of the hypocenters, or the relative location accuracy of neighboring events, is represented by the confidence ellipsoids. The precision of epicenters, expressed in terms of the maximum semi-axis of the projected one-standard-deviation confidence ellipsoid (SEH), averages 4.4, 1.7, and 1.9 km, respectively, in the eastern (east of longitude 145°W.), central (between longitudes 145°E and 150°W.) and western (west of longitude 150°W.) parts of the network. Similarly, the precision of focal depth (SEZ) averages about 4.7, 3.0 and 3.3 km, respectively. The variation in the precision of hypocenter determination across the network is strongly influenced by differences in the station density in the different regions. Hypocenter biases equal to and larger than the dimensions of the confidence ellipsoids are not unlikely as a consequence of the over-simplified velocity models assumed in the preparation of this catalog.

Focal Depths

Previous studies (e.g., Francis and others, 1978; Lilwall and Francis, 1978; Uhrhammer, 1980; and McLaren and Frohlich, 1985) have shown that the accuracy of focal depths for shocks occurring in the vicinity of a seismic network is primarily a function of the geometry of the network, the number of P- and S-phase arrivals read, and the adequacy of the assumed velocity model. Depths are generally more accurate for earthquakes where the distance from the epicenter to the closest station (D1) is less than the calculated focal depth used for events located within the network or on its periphery. The accuracy of focal depths usually increases as the number of S-phase arrivals increases; however, systematic S-phase timing errors (due to mistaken identification of a converted phase as S) or "bad" S picks can degrade focal depth estimation accuracy by several kilometers even when azimuthal coverage is good (Gomberg and others, 1990). Focal depths for shallow (depth less than about 20-30 km) shocks within the southern Alaska network generally are not well constrained due to the relatively large distances between stations and to a lack of knowledge about the velocity structure. Calculated depths for the same event can vary by several kilometers depending on the number of P- and S-phase arrivals used in the location, the trial focal depth, the velocity model, and the P-phase traveltime corrections used to locate the earthquake. Ambiguity in the calculated depth occasionally arises in cases where the traveltimes to receiving stations are similar for upward-leaving rays from a deep source and for downward-leaving rays from a shallow source; this situation leads to double minima in the variation of RMS residuals with depths and is common for events outside the boundaries of the network.

Completeness of Catalog

The magnitude threshold at which this catalog is complete varies geographically as a function of the density of stations and the criteria for timing earthquakes (see section on Data Processing and Appendix C). This catalog contains an early time period for which the seismic data collected by the project were not processed:

November and December 1971
January, February 1-21, and March 2-18, 1972

The most thorough error checking was completed for time periods with published catalogs (Appendix B) and for data processed since 1981. First order quality control checks were made to the catalog for the time periods before 1981.

For some time periods, data from published catalogs from the National Earthquake Information Center (NEIC), the International Seismological Centre (ISC), and/or the Pacific Geoscience Center (PGC) were added to this catalog to improve hypocenter solutions, to facilitate reviews of the seismicity, and to improve the magnitude threshold for completeness. These data typically were added to Alaska network data, and the combined data were rerun with the same velocity models used in routine processing. Some regional events not located by the authors also were included, with hypocenter solutions and phase data taken from other published catalogs.

Seismicity of Southern Alaska

Reviews of the seismicity of the Aleutian arc, continental Alaska, and western Canada have been written by Taber and others (1991), Page and others (1991), and Rogers and Horner (1991), respectively. Meyers (1976) and Espinosa (1984) reviewed teleseismically-recorded earthquakes in Alaska. The purpose of this section is to discuss briefly the distribution of the seismicity within southern Alaska for over 53,000 earthquakes and other events recorded and located by the USGS seismograph network in southern Alaska for October 1971 to May 1989, and to cite the published literature written by the authors. No attempts were made to remove artillery, quarry and mine blasts or glacial quakes from the data set. The gross features of the pattern of seismicity in southern Alaska are shown in Figures 5-9.

The oceanic Pacific plate is being subducted beneath the continental North American plate (Alaska) along the Aleutian megathrust, which crops out on the seafloor at the Aleutian trench (Figure 1). The seismicity related to various tectonic elements can be divided into five distinct source zones as follows: 1) Aleutian megathrust earthquakes along the interface between the subducting Pacific plate and the overriding North American plate; 2) subsea earthquakes within the Pacific plate beneath or seaward of the trench; 3) Wadati-Benioff Zone (WBZ) earthquakes within the subducted part of the Pacific plate landward of the trench; 4) overriding plate earthquakes in the North American plate exclusive of those along the volcanic arc; and 5) volcanic axis earthquakes within the North American plate along the axis of active volcanoes.

Aleutian megathrust earthquakes

Historically, most of the seismic energy in southern Alaska is released in major earthquakes that rupture the shallow part of the dipping thrust between the subducting and overriding plates. In September 1899 a pair of moment magnitude (M_W) 8.1 shocks ruptured the transitional segment between Yakutat Bay and Kayak Island (McCann and others, 1980). In 1964 the convergent plate boundary west of Kayak Island slipped approximately 15 m in a M_W 9.2 earthquake (Plafker, 1969; Hastie and Savage, 1970), the second largest earthquake of the twentieth century worldwide. Beneath a certain depth, estimated to be about 40 km in the Aleutian arc (Davies and House, 1979) and about 20 km in the northern Prince William Sound region (Page and others, 1989), the interface slips aseismically.

The coastal region from about Kayak Island to Yakutat Bay had been identified by the early 1970's as a seismic gap due to the lack of significant shocks since the turn of the century (Tobin and Sykes, 1968; Kelleher, 1970; Sykes, 1971). In 1979, the M_S 7.1 St. Elias earthquake (Figure 5) occurred at the eastern end of this gap and involved low-angle, north-northwest-directed thrusting (Hasegawa and others, 1980) at depths between 10-15 km (Stephens and others, 1980) in a zone that at least locally is no more than 2-3 km thick (Page and others, 1984). The Yakataga seismic gap, which extends westward from the western limit of the St. Elias aftershock zone to the eastern extent of the 1964 rupture, is considered a likely site for a great (M_S 7.8 or greater) thrust earthquake within the next few decades (McCann and others, 1980; Lahr and others, 1980; Jacob, 1984; Stephens and others, 1992).

Seismicity of the gap region has been monitored nearly continuously since 1974 when the network was extended across this region. East of longitude 145°W, the apparent high rate of shallow activity is due at least in part to a lower magnitude threshold used in selecting events for processing. During this period the spatial distribution of seismicity landward of the continental margin has remained relatively stable and is characterized by broad concentrations of shallow seismicity (depths less than 30 km) beneath Icy Bay, Waxell Ridge, and the Copper River delta separated by areas of relative quiescence with most of the shocks occurring in a zone that extends about 90 km inland from the coast (Figure 7 and Figure 9, section D). The most active area has been the aftershock zone of the St. Elias earthquake, both prior to and since the mainshock. Hypocenters of better-recorded shocks from the diffuse patch of seismicity near Waxell Ridge at the center of the gap concentrate near a depth of 12 km (Stephens and others, 1992), which is comparable to the depth to the thrust plane defined by seismicity beneath the St. Elias area. The Copper River Delta seismicity on the western edge of the gap is discussed in the section on Wadati-Benioff zone earthquakes. The largest earthquake located within the gap since 1971 is a M_X 4.1 shock on December 1980 near the southwest corner of the Waxell Ridge concentration of seismicity.

Subsea earthquakes

There is very little historical evidence of seismicity in the Gulf of Alaska seaward of the continental margin. However, in November 1987 and March 1988, two strike-slip earthquakes in the northern Gulf of Alaska with magnitudes M_w 7.9 and M_w 7.8 (respectively) ruptured a composite 250-km-long, north-striking zone in the Pacific plate (Figures 5 and 7) south of the Yakataga seismic gap (Lahr and others, 1988a). These events are thought to reflect shear stress in the Pacific plate seaward of the boundary between the locked Yakataga seismic gap and the recently slipped 1964 rupture.

Wadati-Benioff zone earthquakes

Wadati-Benioff seismic zones are associated with both the northeast-to-north-trending Aleutian volcanic arc west of Cook Inlet and the east-southeast-trending Wrangell volcanic arc east of longitude 145°W. Below 30 km depth the distribution of earthquakes is dominated by activity within the Aleutian Benioff zone west and north of the Cook Inlet region (Figures 5 and 6, and Figure 9, sections C-E). This zone dips west-northwestward from 8-10° beneath the Kenai Peninsula and Anchorage, and then steepens to about 65° west of Cook Inlet, although the latter dip

may be overestimated by about 10-15° due to the systematic bias introduced by using a flat-layered velocity model. Beneath both the southern Kenai Peninsula and Anchorage the upper surface of this zone is at a depth of 30 to 35 km, and beneath the volcanic arc west of Cook Inlet it is at a depth of about 100 km. The average dip of the shallow (depth < 30 km) part of the zone decreases from about 7° beneath Prince William Sound (Page and others, 1991) to about 3-4° beneath the continental margin. On a regional scale using only events with well-constrained focal depths, the maximum thickness of the Aleutian WBZ is about 15 km. The zone appears to thicken slightly beneath the southern Kenai Peninsula and Anchorage. The maximum focal depth varies along the length of the zone from about 200 km near Iliamna (Figure 9, section E) to about 160 km beneath the northernmost Cook Inlet Volcano (Figure 9, section D) and to about 150 km beneath the Alaska Range (Figure 9, section C). Beneath continental Alaska, the Aleutian WBZ is made up of a single zone of earthquakes, in contrast to the two zones of seismicity beneath the eastern Aleutian arc near the Shumagin Islands (Taber and others, 1991). The geometry of the Aleutian WBZ changes along strike as documented in studies of both teleseismically and regionally recorded earthquakes (Van Wormer and others, 1974; Lahr, 1975; Davies, 1975; Agnew, 1980; Pulpan and Frohlich, 1985). In lower Cook Inlet near latitude 59°N, the strike of the deep WBZ rotates 15° counterclockwise (Pulpan and Frohlich, 1985), and about 350 km farther north the strike swings about 35° clockwise (Agnew, 1980). The deeper seismicity east of the Cook Inlet region appears to be bounded by a northwest-southeast trending line, which passes about 50 km northeast of Valdez (Figure 6). Such a line approximately delineates the northeastern terminus of the Aleutian Benioff zone (Stephens and others, 1984a). The diffuse appearance of the Aleutian Benioff zone in Figure 9, section C, may be attributed in part to a lack of focal depth control for earthquakes north of the USGS network (north of 62°N).

The magnitude of the largest shocks recorded by the network within the southern Alaska segment of the Aleutian WBZ since 1971 have been in the magnitude 6 class (Figure 5). In July and September of 1983 the two M_S 6.3 (m_b 6.2) Columbia Bay shocks occurred in the shallow part of the WBZ beneath the north coast of Prince William Sound and involved normal faulting on steeply northwestward-dipping planes between depths of 22-35 km (Page and others, 1985, 1989). A M_X 6.1 (m_b 5.5) earthquake occurred beneath Mt. Spurr in November 1988 with a calculated depth of 138 km. The focal mechanism for this event, using local network data, exhibits down-dip tension and along strike compression which is typical for the deep WBZ zone activity in the Cook Inlet region (Lahr, 1975; Engle, K. Y., 1982; Pulpan and Frohlich, 1985).

The rate and character of seismicity between the shallow and deep parts of the Aleutian WBZ are significantly different, with the higher level of activity in the deep part of the zone beneath the western Kenai Peninsula, Cook Inlet, and the volcanic arc. Since 1971 the distribution of seismicity generally has not been uniform and has a significant component of spatial and temporal clustering. Clustering is more common in the shallow WBZ with mainshocks followed by energetic aftershock sequences such as the aftershock sequences following the two 1983 Columbia Bay earthquakes. In contrast, few, if any, aftershocks have been recorded following WBZ shocks in the deep part. Three persistent, diffuse concentration of events not associated with an aftershock sequence are located about 40 km northeast, 150 km southeast, and 75 km southwest of the Columbia Bay shocks beneath the Tazlina Glacier (latitude 61°N30'N, longitude 146°35'W), the Copper River Delta, and the northern end Knight Island, respectively. The Tazlina Glacier cluster

is a north-northeast-trending swath of seismicity with depths between 25-45 km (Page and others, 1989). Preliminary relocations of well-recorded earthquakes in the persistent, low-magnitude seismicity beneath the Copper River Delta at the western edge of the gap occur at depths between 20-30 km and appear to occur below the megathrust based on one teleseismically recorded thrust event that occurred in 1970 with a depth of about 21 km (Stephens and others, 1992). The northern Knight Island source area was the focus of a special field recording effort in 1987 in which eight stations were operated for one month. Relocated hypocenters from that effort define a subhorizontal tabular zone, which is 6 km thick and whose upper surface is about 18 km deep (Lahr and others, 1988b). Spatial clustering in the deep WBZ is conspicuous (Figures 5 and 6) with concentrations of events deeper than 110 km beneath Mts. Iliamna and McKinley and northwest of Anchorage, while other parts are relatively quiet, such as in the vicinity of the two points 60.8°N, 152.5°W and 62.5°N, 150.2°W.

East of the Aleutian zone lies the weakly active Wrangell WBZ, which dips to the north-northeast beneath the Wrangell volcanoes (Stephens and others, 1984a; Page and others, 1989). This zone extends at least 150 km along strike and to depths of at least 100 km (Figure 6 and Figure 9, sections A and B). The Wrangell WBZ is about two orders of magnitude less active than the Aleutian zone. The largest earthquakes located in this zone by the network are a 4.5 m_b (M_X 3.7) event in September 1986 at a depth of 48 km and a M_X 3.7 shock in February 1989 at a depth of 55 km. The deepest well constrained shock is a M_D 2.4 shock in September 1986 at 97 km depth beneath Mt. Wrangell. The seismicity in the Aleutian and Wrangell zones appears to be continuous, at least in the depth range 20-45 km, and may define adjacent limbs of a buckle in the subducted plate (Page and others, 1989).

Overriding plate earthquakes

Generally the distribution of shallow seismicity within the North American plate away from the volcanic axis since 1971 has been diffuse (Figure 7), and the majority of the events cannot be clearly associated with mapped fault traces. In a few cases, including the Talkeetna segment of the Castle Mountain fault, the Duke River fault near longitude 141°W, and the northernmost segment of the Fairweather fault, earthquakes are closely associated with mapped faults. The diffuse character of the seismicity north of latitude 62.5EN, south of latitude 59.5EN and east of longitude 138°W is at least partially attributed to these areas being outside the USGS seismograph network. The shallow seismicity does has three conspicuous concentrations: 1) a narrow zone parallel to the Duke River fault on the U.S-Canada border, 2) a diffuse north-northeast-trending band of seismicity near longitude 150°W extending between the Denali fault and Cook Inlet whose focal depths lie well above the Aleutian WBZ (Figure 9, section D), and 3) a band north of and parallel to the Castle Mountain fault east of longitude 151°W. To some degree, the apparent scatter of the seismicity near the Duke River fault reflects errors in the epicenters due to uncertainties in the velocity structure and the lack of nearby seismograph stations. Recent shocks located from both regional (Horner, 1983) and local (Power, 1988b) recordings reveal that the seismicity is mostly concentrated in the vicinity of the Duke River fault.

Since 1971 the largest shallow shocks in the overriding plate have been in the magnitude 5 class (Figure 5). The August 1984 m_b 5.7 Sutton earthquake ruptured a 10-km-long buried segment of the Castle Mountain fault and involved right-lateral slip on a steeply north-dipping plane (Lahr

and others, 1986). This is the largest shock to be clearly associated with a mapped fault since the network was established. Two earthquakes, with magnitudes M_X 5.3 (m_b 5.3) and M_X 5.0 (m_b 4.9), occurred 3 days apart about 75 km northwest of Juneau and a few km east of the mapped trace of the Chatham Strait fault. A m_b 5.7 (M_X 5.6) shock occurred in November 1987 on the Duke River fault. The M_X 5.6 (m_b 4.7) shock of March 1989 was located 150 km west of Juneau near the entrance to Cross Sound is about 10 km west of the mapped trace of the Fairweather fault.

Earthquakes with reported depths of 30 km and deeper (Figure 6) east of longitude 145°W (excluding shocks beneath or more than 100 km southwest of the Wrangell Volcanoes), west and north of the Aleutian WBZ generally have poorly constrained focal depths and are probably in the overriding plate.

Volcanic axis earthquakes

Small, shallow earthquakes are abundant along both the Aleutian (Kienle and others, 1983; Stephens and others, 1984b) and Wrangell (Page and others, 1989) volcanic axes. The shocks recorded by the network west of Cook Inlet form a diffuse band, approximately 30 km wide, punctuated by pronounced clusters (Figure 7 and Figure 9, sections D and E). The volcanoes are marked by dense clusters of earthquakes shallower than 5 km, whereas elsewhere along the Aleutian axis shocks fall in the depth range 5 to 20 km (Stephens and others, 1984b).

Both the 1976 and 1986 eruptions of Augustine Volcano in lower Cook Inlet were preceded and accompanied by large numbers of small earthquakes (Lalla and Kienle, 1986; Reeder and Lahr, 1987; Power, 1988). Although the earthquakes associated with these eruptions were too small to be located by the USGS network (and do not appear in the epicenter or cross section plots), the USGS stations were used to monitor activity during the 1986 eruption after all of the stations on the island had failed, possibly due to mudslides (Reeder and Lahr, 1987).

Availability of Data

The summary and corresponding archive arrival time data for over 53,000 earthquakes and other events located by the USGS southern Alaska seismograph network (Table 1) and the HYPOELLIPSE station and control files (UNIX non-Y2K version) used to locate the events are available in this report. These data also include artillery, quarry and mine blasts and glacial quakes as well as readings from teleseismic earthquakes and nuclear explosions used to check 1st motion polarities of seismograph stations (see Table 5). Appendix B lists previously published catalogs available from the USGS Store, *http://store.usgs.gov*, 1-888-275-8747.

Acknowledgements

We thank the former chiefs (Howell Butler, Robert Eppley, and Tom Sokolowski) of the NOAA Tsunami Warning Center, as well as the staff and members, including Wayne Jorgensen, Alex Medbery, John Sindorf, and George Carte, for their assistance in maintaining our recording equipment in Palmer, Alaska, as well as making their seismic data available to us.

We thank Juergen Kienle, Niren Biswas, Steve Estes, John Benevento and the staff of the Geophysical Institute of the University of Alaska for exchange of seismic data and cooperation in the operation of southern Cook Inlet seismograph stations.

We are indebted to over fifteen seismic data analysts who routinely processed the data since 1971, most of whom worked on the project for less than five years. We especially wish to thank Roy Tam who has been with the project since 1979.

We are indebted to the project's engineer, John Rogers, and all of those who have spent time fabricating, installing, and maintaining the seismograph network in Alaska, especially Mike Blackford and Ed Criley.

References

Agnew, J.D., 1980, Seismicity of the central Alaska Range, Alaska, 1904-1978, Master's thesis, Fairbanks, University of Alaska, 88 p.

Astrue, M.C., Pelton, J.R., Lee, W.H.K., and Page, R.A., 1983, Operator's manual for a four-film computer based , sonic digitizing table to locate earthquakes, U.S. Geological Survey Open-File Report 83-319, 40 p.

Davies, J.N., 1975, Seismological investigations of plate tectonics in south-central Alaska, Ph.D. thesis, Fairbanks, University of Alaska, 193 p.

Davies, J.N., and House, L., 1979, Aleutian subduction zone seismicity, volcano-trench separation, and their relation to great thrust-type earthquakes, Journal of Geophysical research, v. 84, p. 4583-4591.

Eaton, J.P., O'Neill, M.E., and Murdock, J.N., 1970, Aftershocks of the 1986 Parkfield-Cholame, California, earthquake: a detailed study, Bulletin of the Seismological Society of America 60, p. 1151-1197.

Engle, K.Y., 1982, earthquake focal mechanism studies of Cook Inlet area, Alaska, Master's thesis, Fairbanks, University of Alaska, 81 p.

Espinosa, A.F., 1984, Seismicity of Alaska and the Aleutian Islands, 1960-1983, U.S. Geological Survey Open-File Report 84-855, 1 over-size sheet, scale 1:12,500,000.

Fogleman, K.A., and Rogers, J.A., 1987, ELOG: Design and development of a digital earthquake recorder in study of the 1986 Talkeetna, Alaska earthquake swarm: Seismological Research Letters, Eastern Section - Seismological Society of America, v. 58, no. 1, p. 12.

Francis, T.J.G., Porter, I.T., and Lilwall, R.C., 1978, Microearthquakes near the eastern end of St. Pauls Fracture Zone, Geophysical Journal Royal Astronomical Society, v. 53, p. 201-217.

Gomberg, J.S., Shedlock, K.M., and Roecker, S.W., 1990, The effect of S-wave arrivals times on the accuracy of hypocenter estimation, Bulletin of the Seismological Society of America, v. 80, no. 6, p. 1605-1628.

Hasegawa, H.S., Lahr, J.C. and Stephens, C.D., 1980, Fault parameters of the St. Elias, Alaska, earthquake of February 28, 1979, Bulletin of the Seismological Society of America, v. 70, no. 5, p. 1651-1660.

Hastie, L.M., and Savage, J.C., 1970, A dislocation model for the 1964 Alaska earthquake, Bulletin of the Seismological Society of America, v. 60, p. 1389-1392.

Horner, R.B, 1983, Seismicity in the St. Elias region of northwestern Canada and southeastern Alaska, Bulletin of the Seismological Society of America, v. 73, p. 1117-1137.

Jacob, K.H., 1972, Global tectonic implications of anomalous seismic P traveltimes from the nuclear explosion Longshot, Journal of Geophysical Research 77, p. 2556-2573.

Jacob, K.H., 1984, Estimates of long-term probabilities for future great earthquakes in the Aleutians, Geophysical Research Letters, v. 11, p. 295-298.

King, P.B., compiler, 1969, Tectonic Map of North America, U.S. Geological Survey, scale 1:5,000,000.

Kelleher, J.A., 1970, Space-time seismicity of the Alaska-Aleutian seismic zone, Journal of Geophysical research, v. 75, p. 5745-5756.

Kienle, J., Swanson, S.E., and Pulpan, H., 1983, Magmatism and subduction in the eastern Aleutian arc, *in* Shimozuru, D., and Yokoyama, I., eds, Arc volcanism, Physics and tectonics, Terra Scientific Publishing Company, p. 191-224.

Lahr, J.C., 1975, Detailed seismic investigation of Pacific-North American plate interaction in southern Alaska, Ph.D. dissertation, Columbia University, 141 p.

Lahr, J.C., 1989, HYPOELLIPSE/Version 2.0: A computer program for determining local earthquake hypocentral parameters, magnitude, and first-motion pattern, U.S. Geological Survey Open-File Report 89-116, 60 p. *http://pubs.usgs.gov/of/1989/0116/report.pdf*

Lahr, J.C., 1999, HYPOELLIPSE: A computer program for determining local earthquake hypocentral parameters, magnitude, and first-motion pattern, (Y2K Compliant Version), U.S. Geological Survey Open-File Report 99-23, 116 p. *http://pubs.usgs.gov/of/1999/ofr-99-0023/*

Lahr, J.C., Engdahl, E.R., and Page, R.A., 1974, Locations and focal mechanisms of intermediate depth earthquakes below Cook Inlet, Alaska, EOS 55, 349 p.

Lahr, J.C., George Plafker, C.D.Stephens, K.A. Fogleman, and M.E. Blackford, 1979, Interim report on the St. Elias, Alaska earthquake of 28 February 1979, U.S. Geological Survey Open-File Report 79-670, 35 p. Also *in* Earthquake Engineering Research Institute Newsletter, v. 13, no. 4, p. 54-76.

Lahr, J.C., Page, R.A., Stephens, C.D., and Fogleman, K.A., 1986, Sutton, Alaska, earthquakes of 1984: Evidence for activity on the Talkeetna segment of the Castle Mountain fault system, Bulletin of the Seismological Society of America, v. 76, no. 4, p. 967-983.

Lahr, J.C., Page, R.A., Stephens, C.D., 1988a, Unusual earthquakes in the Gulf of Alaska and fragmentation of the Pacific plate, Geophysical Research Letters, v. 15, no. 13, p. 1483-1486.

Lahr, J.C., and Stephens, C.D., 1983, Eastern Gulf of Alaska seismicity: final reports to the National Oceanic and Atmospheric Administration for July 1, 1975 through September 30, 1981: U.S. Geological Survey Open-File Report 83-592, 48 p.

Lahr, J.C., Stephens, C.D., Hasegawa, H.S., and Boatwright, J., 1980, Alaskan seismic gap only partially filled by 28 February 1979 earthquake, Science, v. 207, p. 1351-1353.

Lahr, J.C., Stephens, C.D., Page, R.A., and Fogleman, K.A., 1988b, Alaska seismic studies, National Earthquake Hazards Reduction Program Summaries of Technical Reports, v. 25, U.S. Geological Survey Open-File Report 88-66, p. 16-24.

Lalla, D.J., and Kienle, J., 1986, Seismic and thermal precursors to the January 1976 eruption of Augustine Volcano, Alaska, abstract, Auckland, New Zealand, International Volcanological Congress, February 1986, p 251.

Lee, W.H.K., Bennett, R.E., and Meager, K.L., 1972, A method of estimating magnitude of local earthquakes from signal duration, U.S. Geological Survey Open-File Report, 28 p.

Lee, W.H.K., and Lahr, J.C., 1972, HYPO71: a computer program for determining hypocenter, magnitude, and first motion pattern of local earthquakes, U.S. Geological Survey Open-File Report, 100 p.

Lilwall, R.C., and Francis, T.J.G., 1978, Hypocentral resolution of small ocean bottom seismic networks, Geophysical Journal Royal Astronomical Society, v. 54, p. 721-728.

Matumoto, T., and Page, R.A., 1969, Microaftershocks following the Alaska earthquake of 28 March 1964 -- Determination of hypocenters and crustal velocities in the Kenai Peninsula-Prince William Sound area, in Wood, F.J., ed., The Prince William Sound Earthquake of 1964 and Aftershocks, v. II, Parts B and C, U.S. Coast and Geodetic Survey Publication 10-3, U.S. Government Printing Office, Washington, D.C., p. 157-173.

McCann, W.R., Perez, O.J., and Sykes, L.R., 1980, Yakataga seismic gap, southern Alaska: Seismic history and earthquake potential: Science, v. 207, p. 1309-1314.

McLaren, J.P., and Frohlich, C., 1985, Model calculations of regional network locations for earthquakes in subduction zones, Bulletin of the Seismological Society of America, v. 75, no. 2, p. 397-413.

Meyers, H., 1976, A historical summary of earthquake epicenters in and near Alaska, NOAA Technical Memorandum EDS NGSDC-1, 57 p.

Mitronovas, W., and Isacks, B.L., 1971, Seismic velocity anomalies in the upper mantle beneath the Tonga-Kermadec island arc, Journal of Geophysical Research 76, p. 7154-7180.

Page, R.A., Hassler, M.H., Stephens, C.D., and Criley, E.E., 1984, Fault zone geometry of the 1979 St. Elias, Alaska, earthquake, *in* The United States Geological Survey in Alaska: Accomplishments during 1982, U.S. Geological Circular 939, p. 65-67.

Page, R.A., Stephens, C.D., Fogleman, K.A., and Maley, R.P., 1985, The Columbia Bay, Alaska, earthquakes of 1983, *in* Bartsch-Winkler, Susan, and Reed, K.M., eds., The United States Geological Survey in Alaska, Accomplishments during 1983, U.S. Geological Survey Circular 945, p. 80-83.

Page, R.A., Plafker, George, Fuis, G.S., Nokleberg, W.J., Ambos, E.L., Mooney, W.D., and Campbell, D.L., 1986, Accretion and subduction tectonics in the Chugach Mountains and Copper River Basin, Alaska: initial results of the Trans-Alaska Crustal Transect, Geology, v. 14, p. 501-505.

Page, R.A., Stephens, C.D., and Lahr, J.C., 1989, Seismicity of the Wrangell and Aleutian Wadati-Benioff zones and the North American Plate along the Trans-Alaska Crustal Transect, Chugach Mountains and Copper river basin, southern Alaska, Journal of Geophysical Research, v. 94, p. 16059-16082.

Page, R.A., Biswas, N.N., Lahr, J.C., and Pulpan, H., 1991, Seismicity of continental Alaska, *in* Slemmons, D.B., Engdahl, E.R., Zoback, M.D., and Blackwell, D.D., eds., Neotectonics of North America: boulder, Colorado, Geological Society of America, Decade Map Volume 1.

Plafker, George, 1967, Geologic map of the Gulf of Alaska Tertiary Province, Alaska, U.S. Geological Survey Miscellaneous Investigations Map I-84, scale 1:500,000.

Plafker, George, 1969, Tectonics of the March 27, 1964, Alaska earthquake, U.S. Geological Survey Professional Paper 543-I, 74 p.

Power, John, 1988a, Seismicity associated with the 1986 eruption of Augustine volcano, Alaska, Master's thesis, Geophysical Institute, University of Alaska, Fairbanks, 142. p.

Power, M.A., 1988b, Mass movement, seismicity, and neotectonics in the northern St. Elias Mountains, Yukon, Master's thesis,, Edmonton, University of Alberta, 125 p.

Pulpan, H., and Frohlich, C., 1985, Geometry of the subducted plate near Kodiak Island and the lower Cook Inlet, Alaska, determined from relocated earthquake hypocenters: Bulletin of the Seismological society of America, v. 75, p. 791-810.

Reeder, J.W., and Lahr, J.C., 1987, Seismological evidence of the 1976 eruption of Augustine volcano, Alaska, U.S. Geological Survey Bulletin 1768, v. 67, no. 44, p. 1197-1198.
Richter, C.F., 1958, Elementary Seismology, W.H. Freeman and Co., San Francisco, Calif., 768 p.
Robinson, M., 1990, Xpick user's manual v 2.7: Seismology Lab, Geophysical Institute**,** University of Alaska, 93 p.
Rogers, G.C., and Horner, R.B., 1991, An overview of western Canadian seismicity, *in* Slemmons, D.B., Engdahl, E.R., Zoback, M.D., and Blackwell, D.D., eds., Neotectonics of North America: Boulder, Colorado, Geological Society of America, Decade Map Volume 1.
Rogers, J.A., 1986, Increasing dynamic range in analog seismic data systems used in Alaska, U.S. Geological Survey Open-File Report, 86-78, 16 p.
Rogers, J.A., 1993, XDETECT version 3.18 users reference guide, U.S. Geological Survey Open-File Report 93-261-A, 27 p.
Rogers, J.A., Maslak, S., and Lahr, J.C., 1980, A seismic electronic system with automatic calibration and crystal reference, U.S. Geological Survey Open-File Report 80-324, 130 p.
Rogers, J.A., and Lahr, J.C., 1986, An on-site seismic data recording system, U.S. Geological Survey Open-File Report 86-251, 47 p.
Stephens, C.D., Lahr, J.C., Fogleman, K.A., and Horner, R.B., 1980, The St. Elias, Alaska, earthquake of 28 February 1979: regional recording of aftershocks and short-term pre-earthquake seismicity, Bulletin of the Seismological Society of America, v. 70, no. 5, p. 1607-1633.
Stephens, C.D., Fogleman, K.A., Lahr, J.C., and Page, R.A., 1984a, Wrangell Benioff zone, southern Alaska, Geology, v. 12, p. 373-376.
Stephens, C.D., Lahr, J.C., and Page, R.A., 1984b, Seismicity along southern coastal Alaska, October 1981-September 1982, *in* Bartsch-Winkler, S., and Reed, K.M., eds., The United States Geological Survey in Alaska, Accomplishments during 1982, U.S. Geological Survey Circular 939, p. 78-82.
Stephens, C.D., Lahr, J.C., Page, R.A., and Fogleman, K.A., 1992, Recent Seismicity in and near the Yakataga seismic gap, southern Alaska, 1992, Abstract, Wadati Conference on great subduction earthquakes, Fairbanks, Alaska, 16-19 September 1992.
Stevenson, P.R., 1978, Program ISDS an interactive display for displaying and measuring seismic waves forms, U.S. Geological Survey-Open File Report 79-205, 175 p.
Sykes, L.R., 1971, Aftershock zones of great earthquakes, seismicity gaps, and earthquake prediction for Alaska and the Aleutians, Journal of Geophysical Research, v. 76, p. 8021-8041.
Taber, J.J., Billington, S., and Engdhal, E.R., 1991, Seismicity of the Aleutian Arc, *in* Slemmons, D.B., Engdahl, E.R., Zoback, M.D., and Blackwell, D.D., eds., Neotectonics of North America: Boulder, Colorado, Geological Society of America, Decade Map Volume 1.
Tobin, D.G., and Sykes, L.R., 1968, Seismicity and tectonics of the northeast Pacific Ocean, Journal of Geophysical Research, v. 73, p. 3821-3845.
Uhrhammer, R.A., 1980, Analysis of small seismographic station networks, Bulletin of the Seismological Society of America, v. 70, no. 4, p. 1369-1379.
Van Wormer, J.D., Davies, J., and Gedney, L., 1974, Seismicity and plate tectonics in south central Alaska, Bulletin of the Seismological Society of America, v. 64, p. 1467-1475.

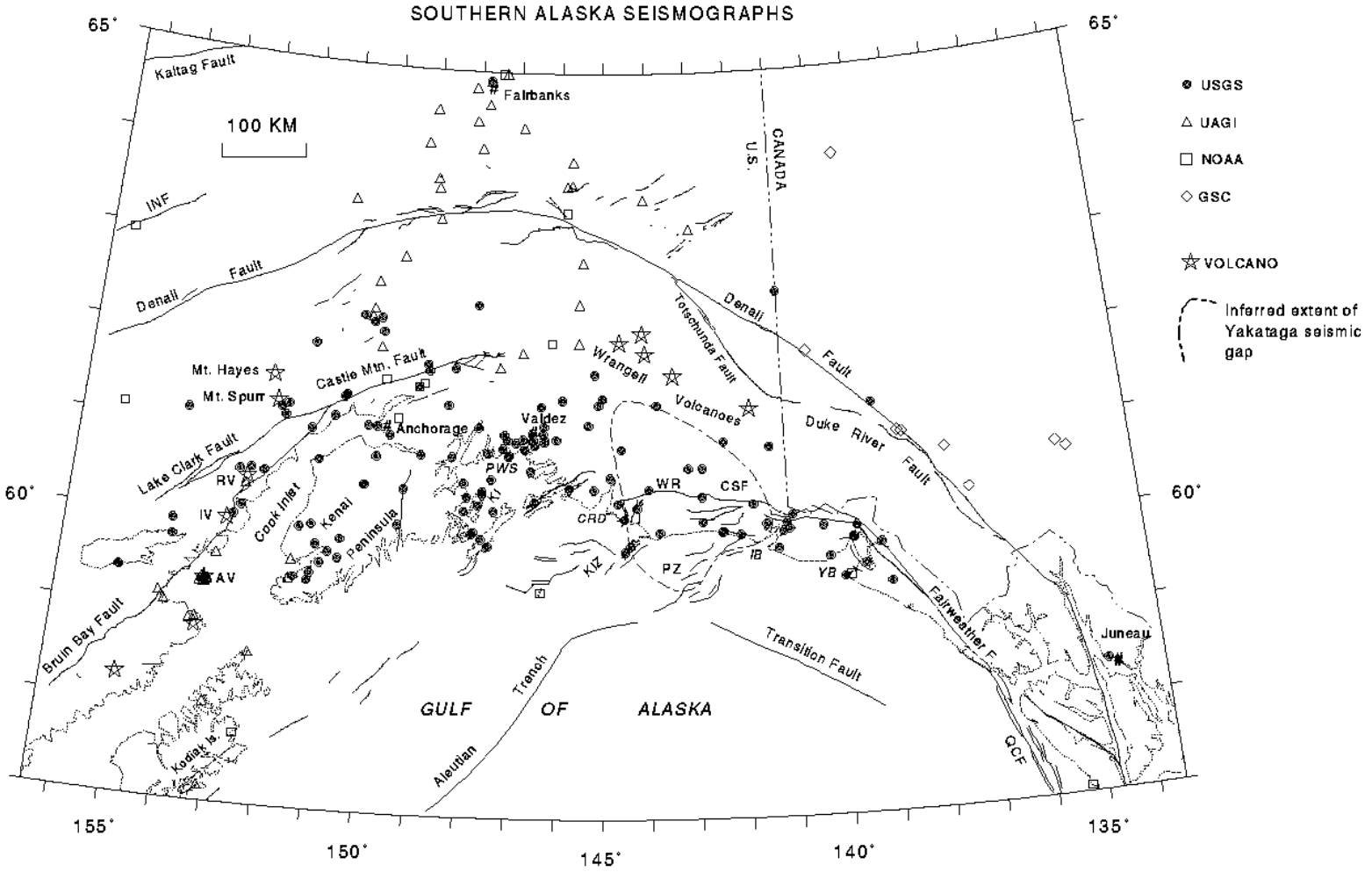

Figure 1. Map showing the locations of all USGS seismograph stations in southern Alaska along with stations operated by other institutions used in the preparation of this catalog. Neogene and younger faults (George Plafter, personal communication, 1988) are shown as solid lines. AV, Augustine volcano; CSF, Chugach-St Elias fault; CRD, Copper River Delta; IB, Icy Bay; IV, Iliamna volcano; INF, Iditarod-Nixon fault; KI, Knight Is; KIZ, Kayak Is Zone; PWS, Prince William Sound; PZ, Pamplona Zone; PWS, Prince William Sound; QCF, Queen Charlotte fault; RV, Redoubt volcano; WR, Waxell Ridge; YB, Yakutat Bay. Quaternary volcanoes are indicated by stars.

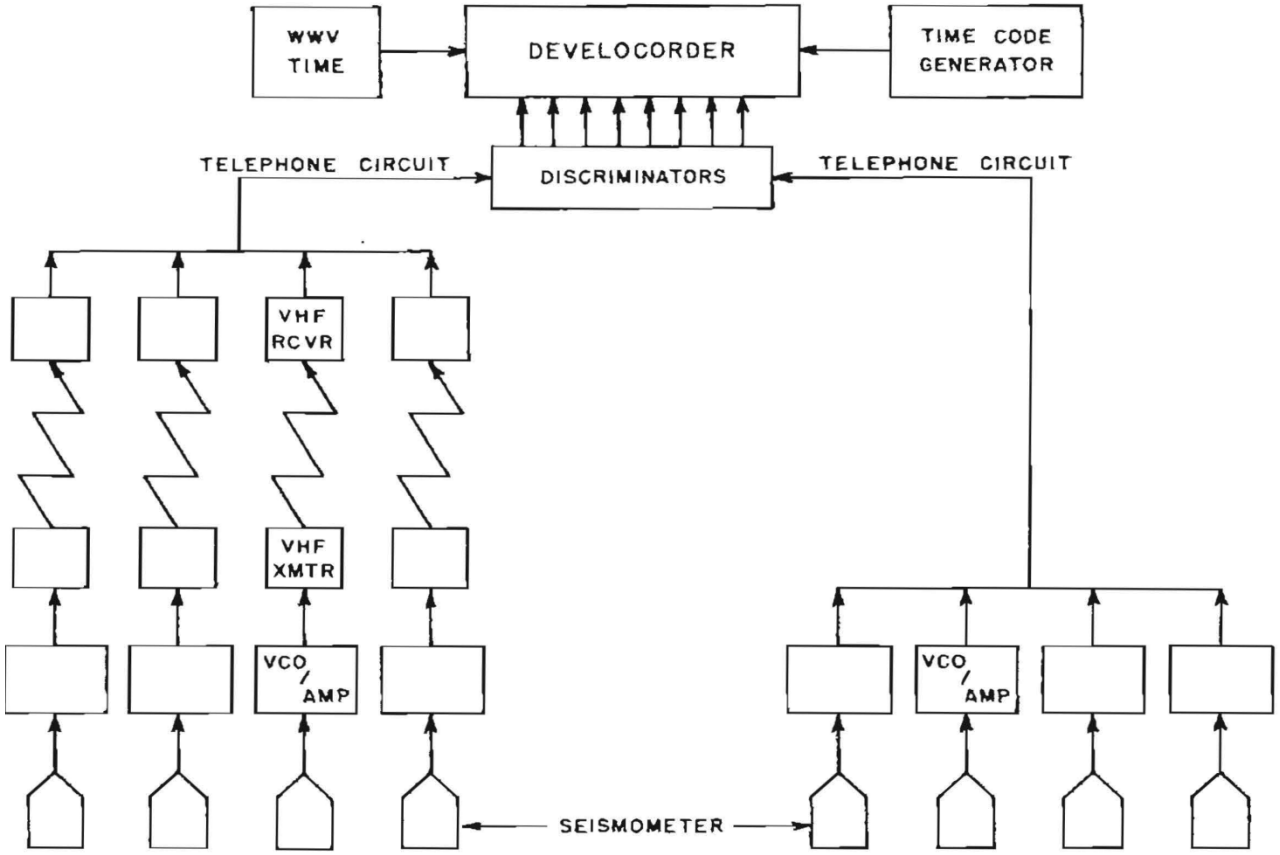

Figure 2. Block diagram of telemetered seismograph system in the USGS Alaska seismic network.

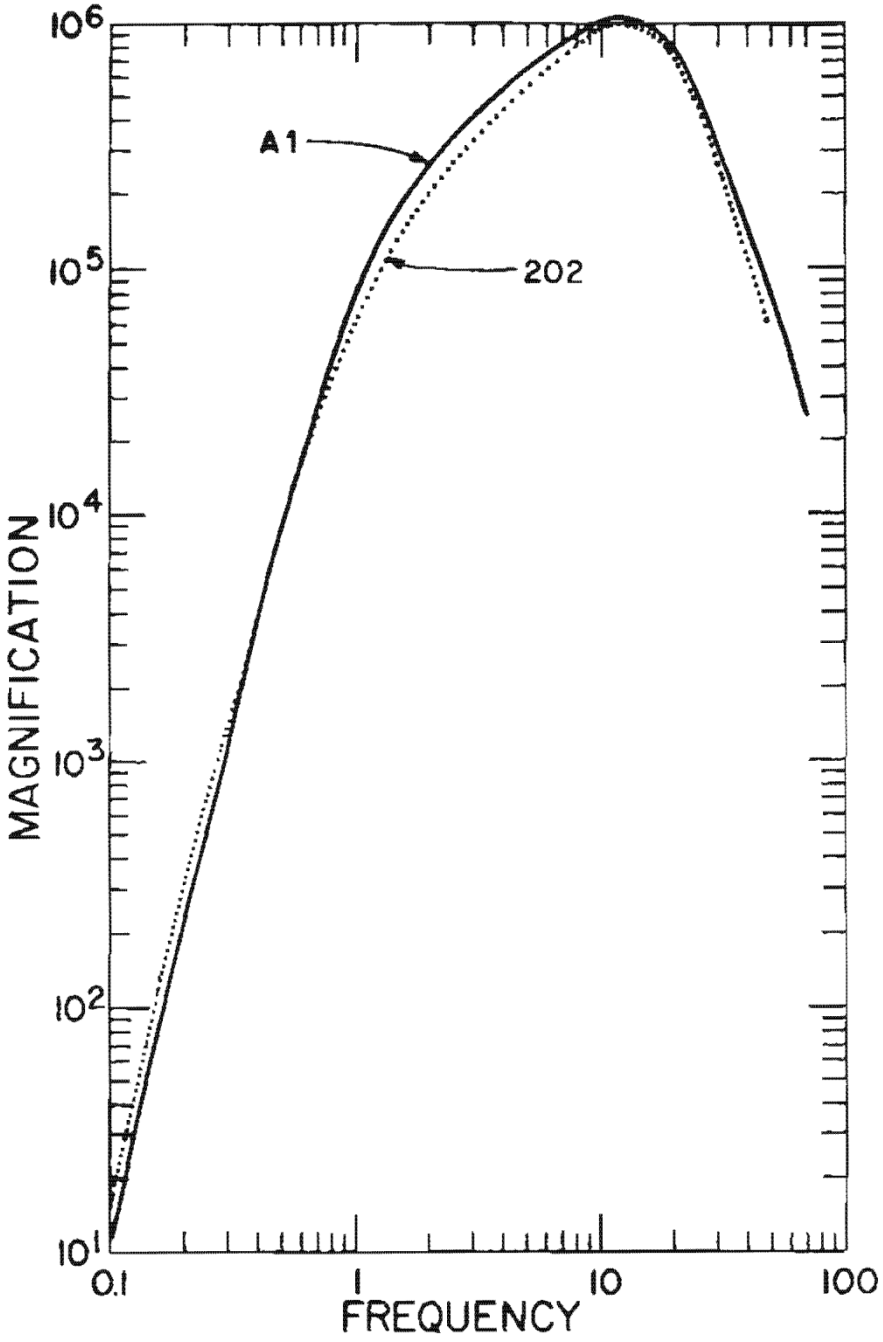

Figure 3. System response curves for typical USGS seismographs that incorporate the A1VCO unit (solid curve) and the older VCO model NCER 202 unit (dotted curve).

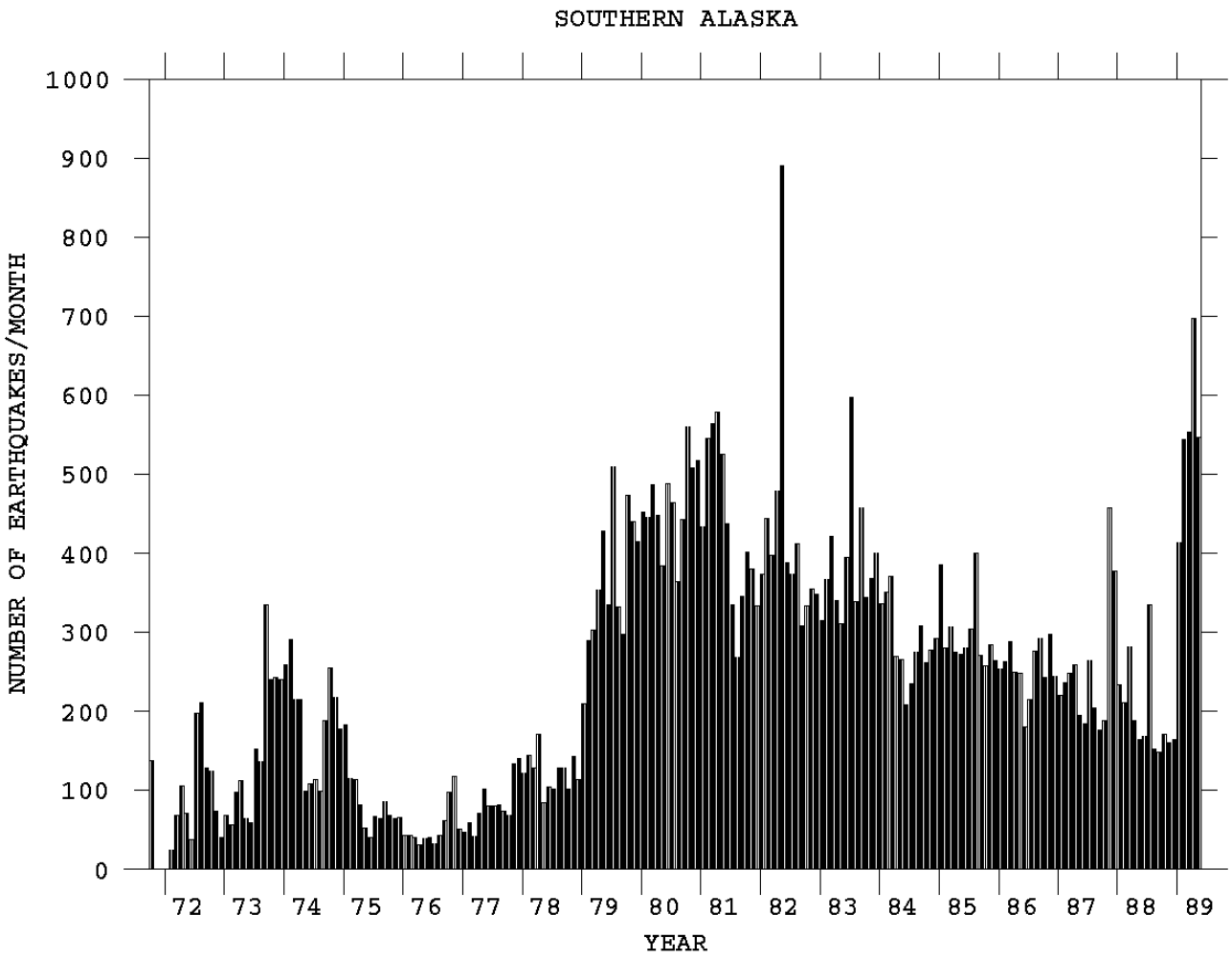

Figure 4. Histogram showing the number of earthquakes per month between October 1971 and May 1989.

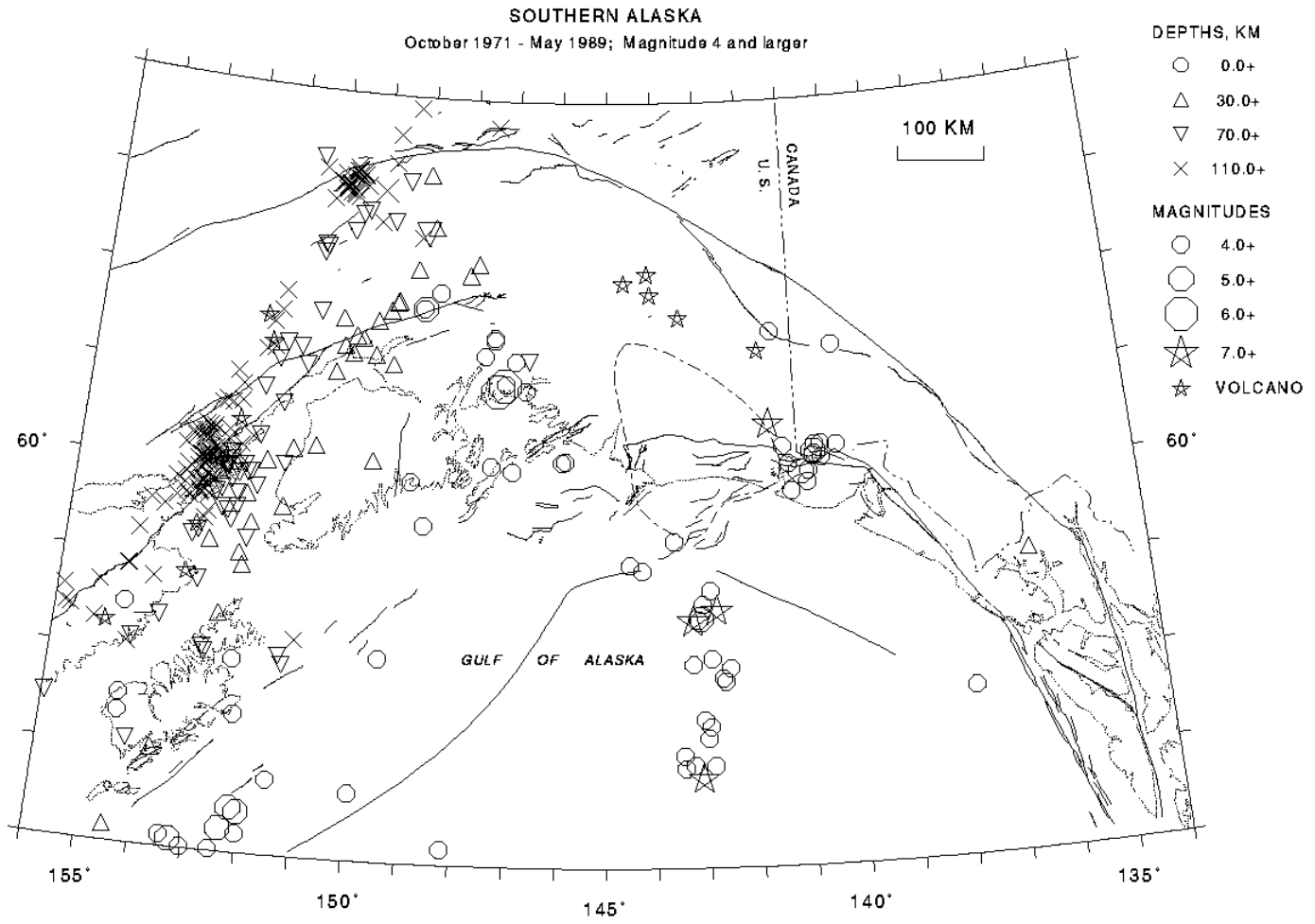

Figure 5. Epicenters of 377 earthquakes of magnitude of 4.0 or larger that occurred between October 1971 and May 1989. See Figure 1 for identification of map features.

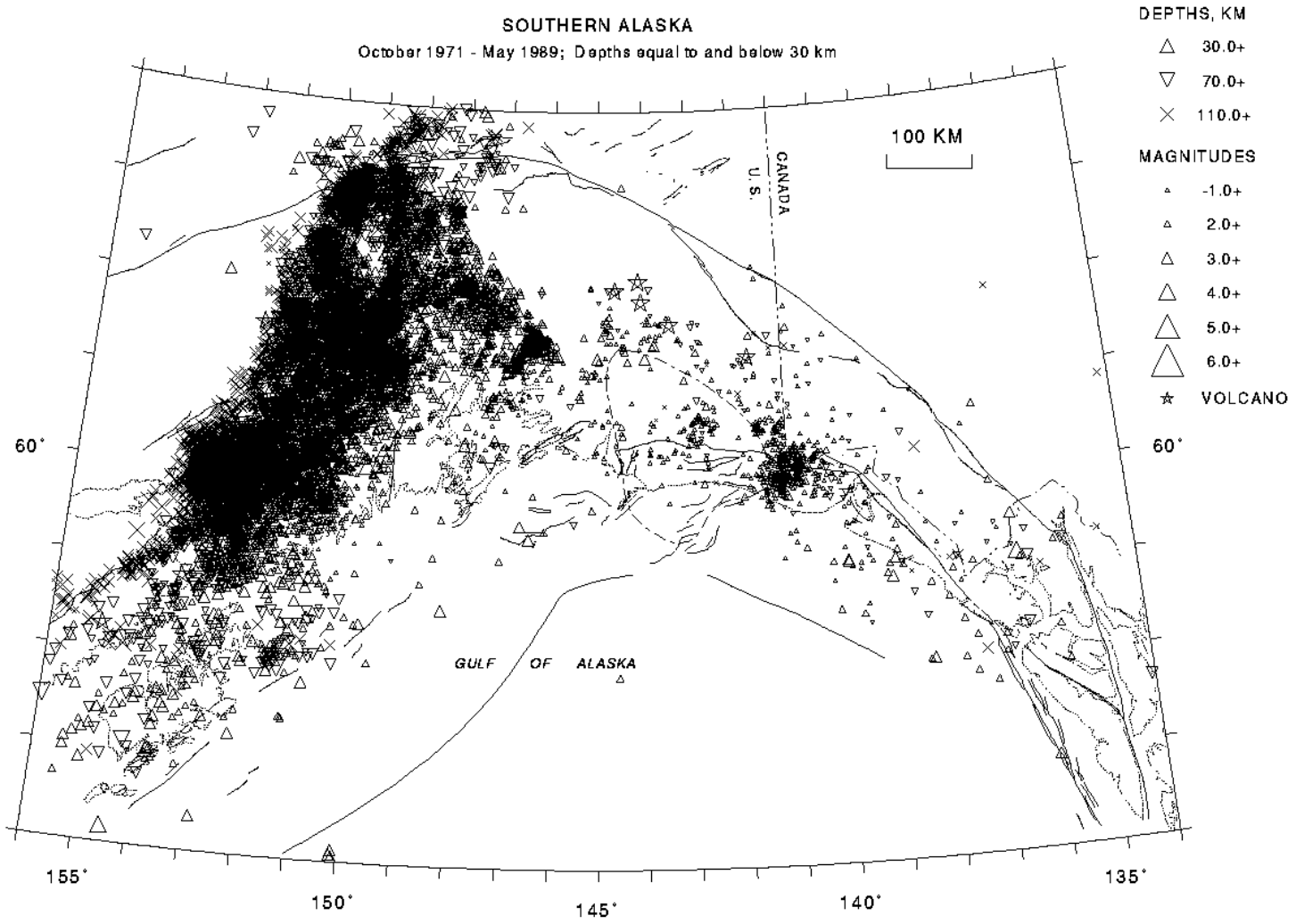

Figure 6. Epicenters of 14,884earthquakes with depths equal to or deeper than 30 km between October 1971 and May 1989.

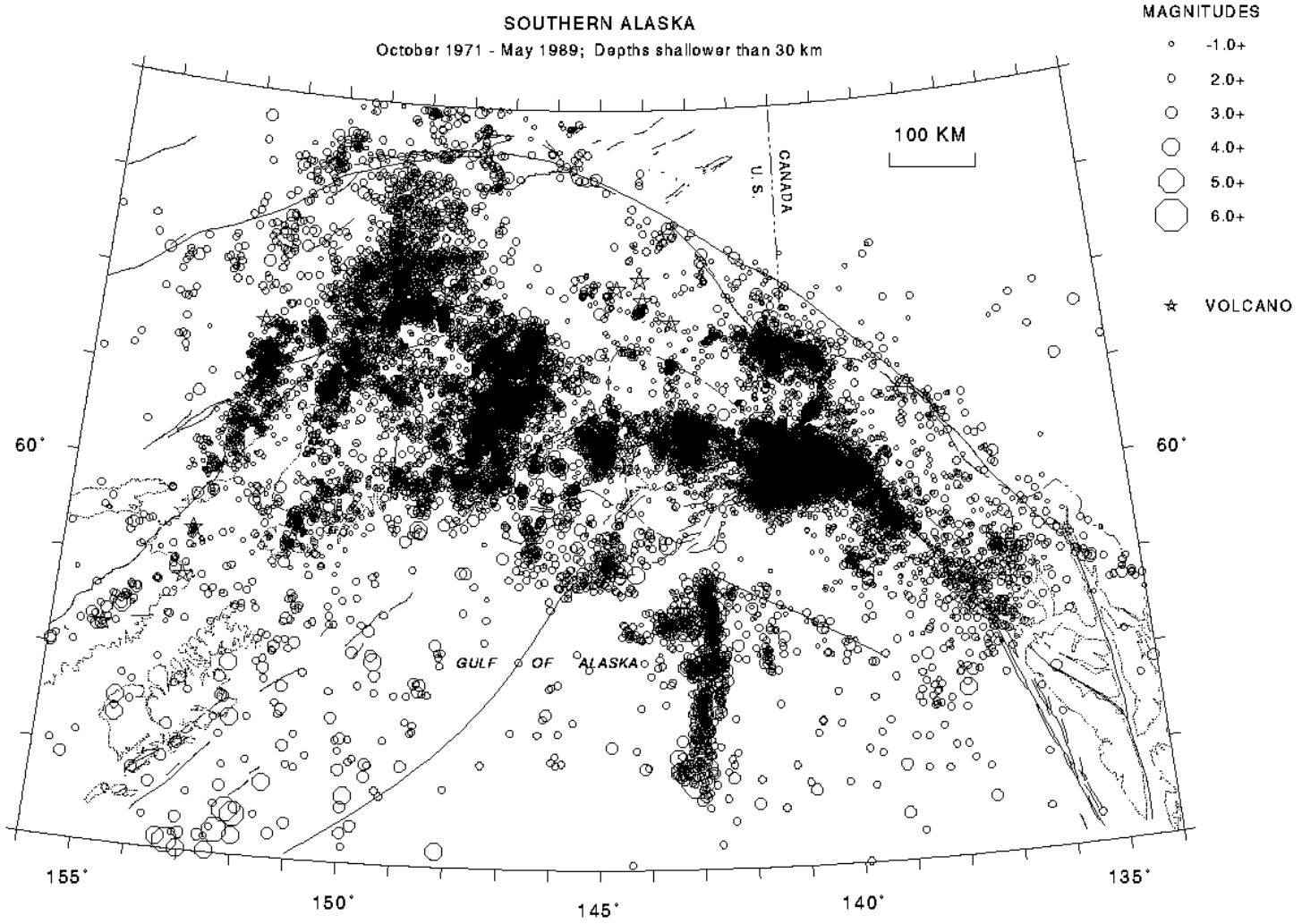

Figure 7. Epicenters of 35,225 earthquakes with depths shallower than 30 km between October 1971 and May 1989.

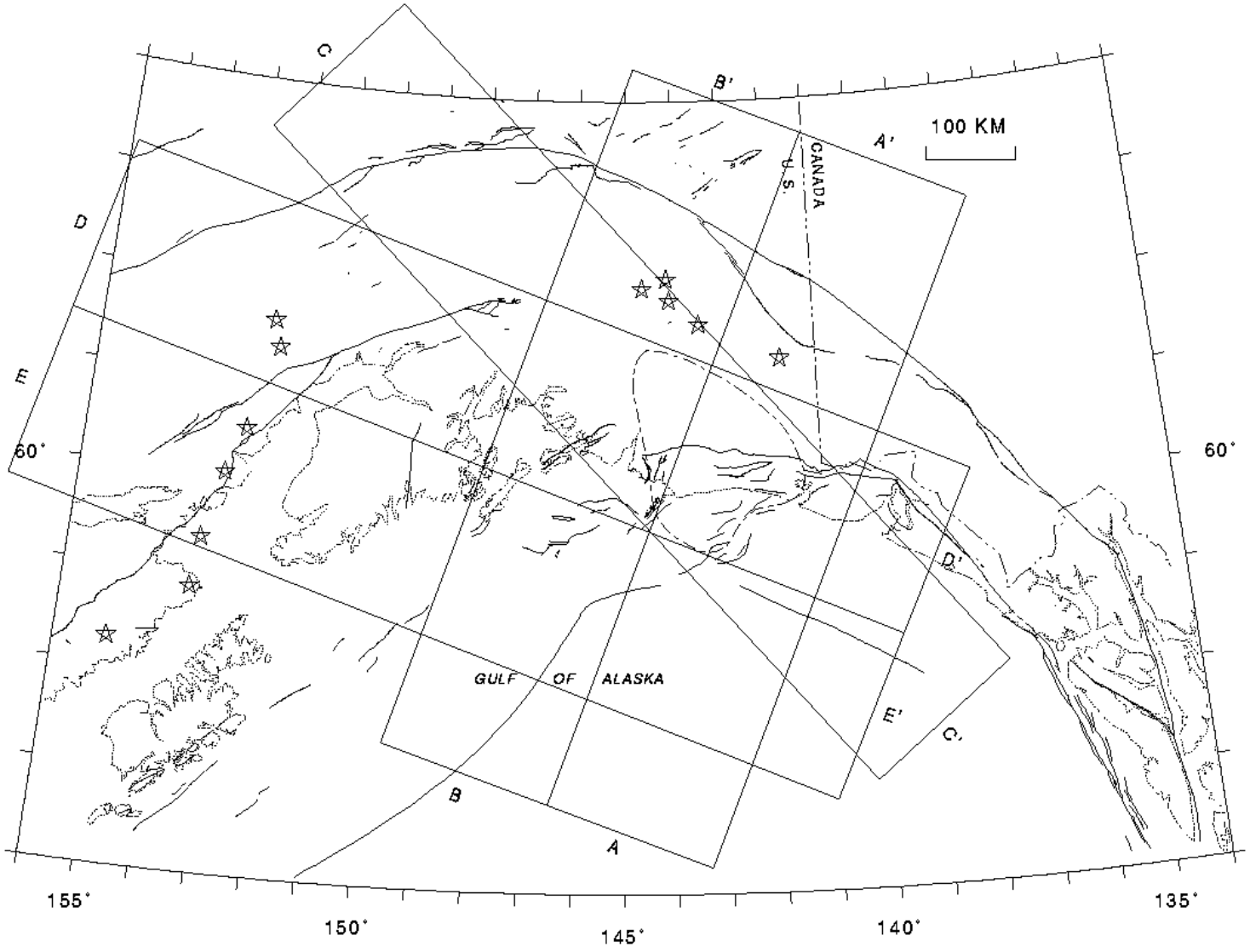

Figure 8 Reference map showing the areas represented in the cross sections in Figure 9.

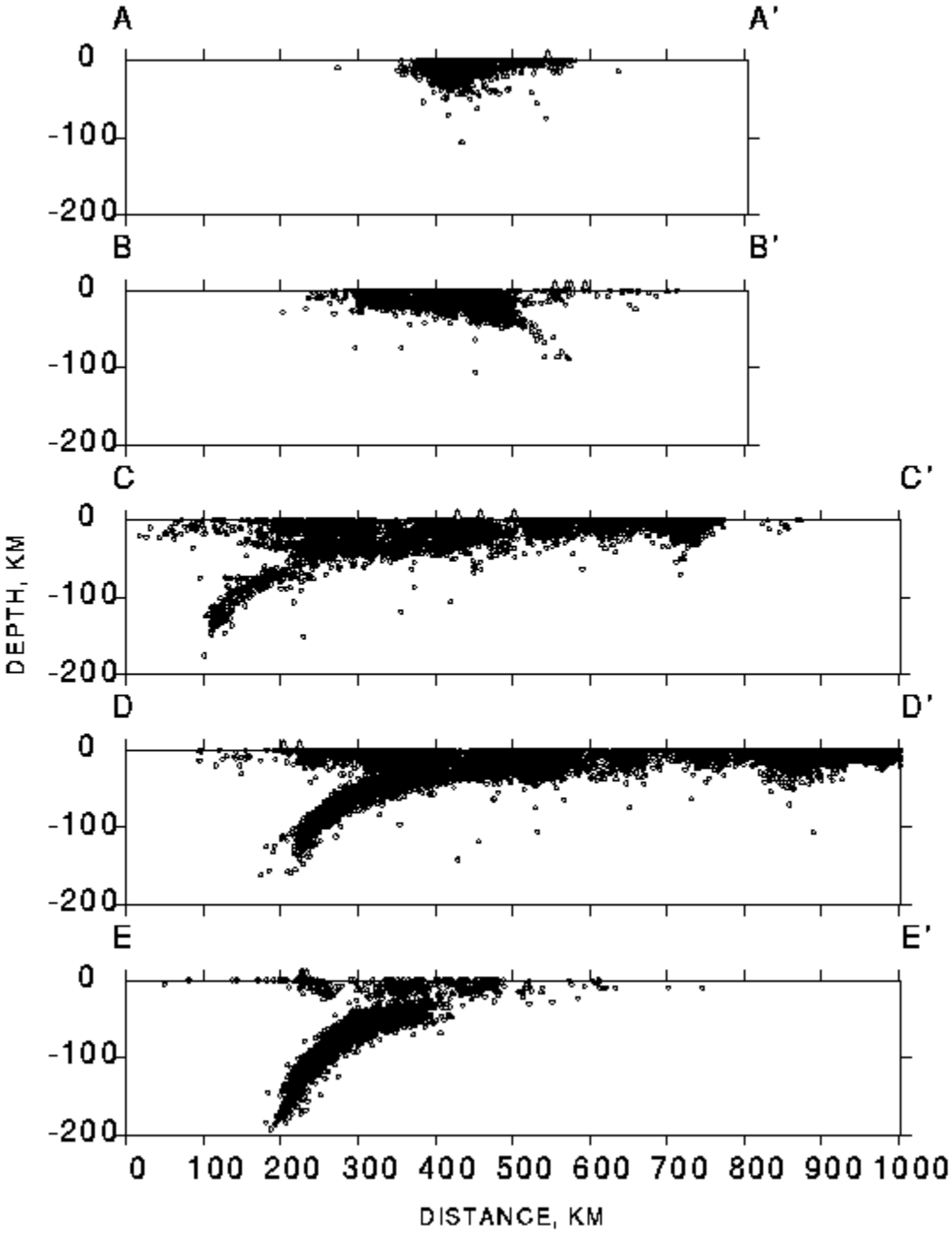

Figure 9. Sections of better-constrained hypocenters (SEH ≤ 5 km and SEZ ≤ 10 km) for areas indicated in Figure 8. Quaternary volcanoes plotted as triangles above zero depth. No vertical exaggeration.

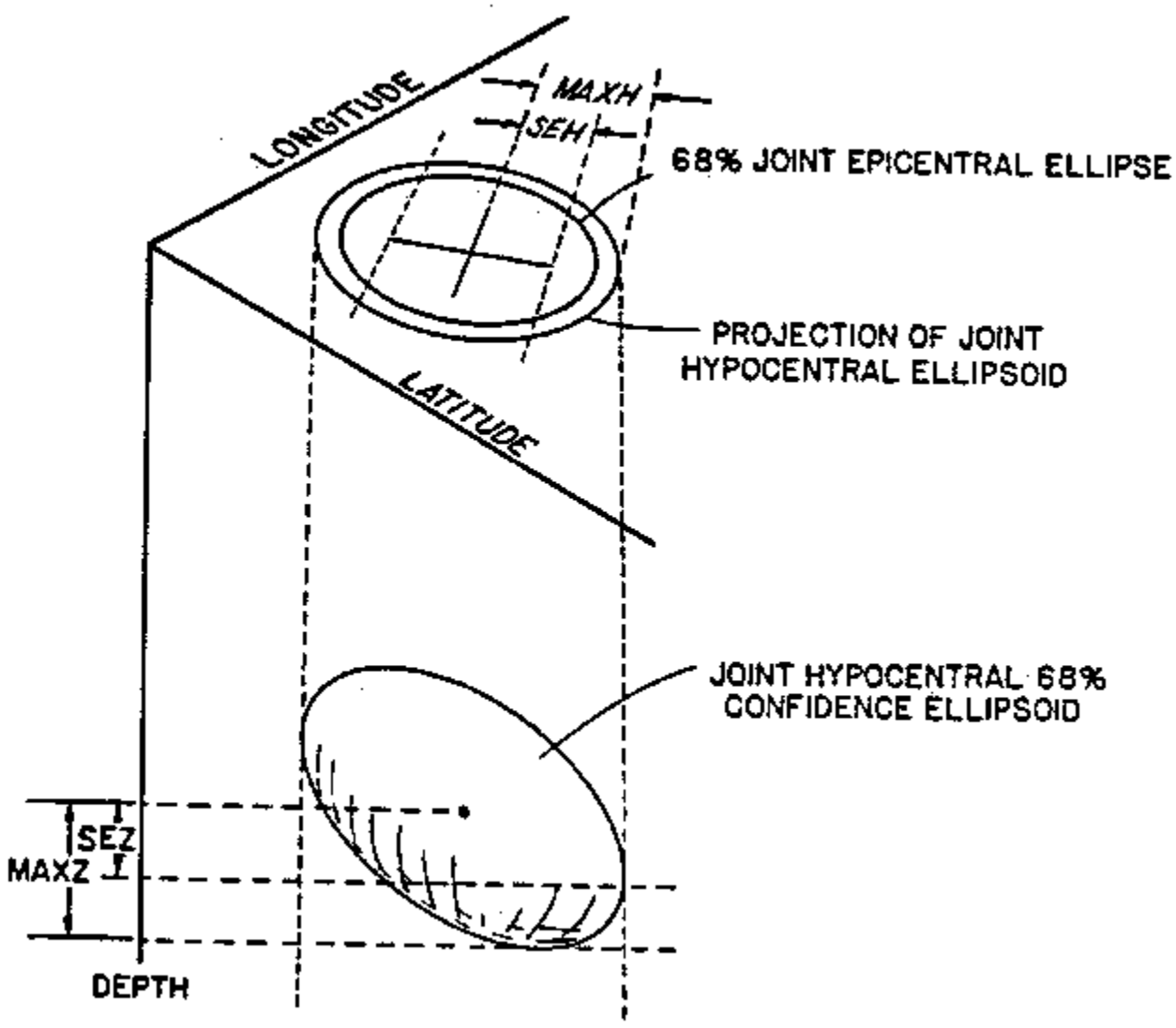

Figure 10. Relationship between the confidence ellipsoid and SEH, MAXH, SEZ, and MAXZ. The projected ellipse has the same orientation and eccentricity as the joint epicentral 68-percent confidence region, but is 1.23 times larger. The error ellipsoid is calculated assuming a constant standard deviation of 0.1 sec for the arrival time readings.

TABLE 1. Stations used to determine hypocenter parameters reported in this catalog. Coordinates are referenced to NAD27 Datum. INST - principal operating institution: USGS - U.S. Geological Survey; UAGI - Geophysical Institute, University of Alaska; NOAA - National Oceanic and Atmospheric Administration, Alaska Tsunami Warning Center, Palmer; GSC - Geological Survey of Canada, Pacific Geoscience Center (formerly Energy Mines and Resources, Canada) . Open date left blank (or = 0) if unknown; closed date left blank if operation continued after May 1989. Asterisk (*) three-component site during at least part of the operation period.

Code	Site Name	Latitude	Longitude	Elev m	INST	Opened	Closed
ABF	Auke Bay	58.3813	-134.6433	3	USGS	80/07/21	
ADK	Adak	51.8837	-176.6845	116	NOAA	66/01/00	
AG1	Augustine Island	59.3800	-153.4200	580	UAGI	71/08/00	76/01/00
AGA	Agassiz Lakes	60.1542	-141.0333	1024	USGS	83/10/05	88/08/26
AGI	Augustine Island	59.3800	-153.4200	580	UAGI	71/08/00	76/01/00
ALC	Alcan	62.6225	-141.0083	582	USGS	79/10/25	82/09/21
ANM	Anvil Mountain	64.5767	-165.3713	323	UAGI	76/09/00	
ANV	Anvil Mountain	64.5600	-165.3713	323	UAGI	76/09/00	
AU1	Augustine Island	59.3732	-153.4205	494	UAGI	71/08/00	76/01/00
AU2	Augustine Island	59.3702	-153.3782	195	UAGI		76/01/00
AU4	Augustine Island	59.3360	-153.5128	18	UAGI	76/01/00	76/01/00
AU5	Augustine Island	59.3865	-153.4558	152	UAGI		76/01/00
AUE	Augustine East	59.3590	-153.3722	172	UAGI	88/10/01	
AUF	Augustine Flow	59.3878	-153.4575	165	UAGI	77/07/28	80/08/25
AUH	Augustine Dome H	59.3638	-153.4435	900	UAGI	92/08/26	
*AUI	Augustine Island	59.3352	-153.4277	293	UAGI	78/01/01	
AUK	Augustine Island	59.3342	-153.4270	293	UAGI	76/10/17	78/04/06
AUL	Augustine Lava Flow	59.3822	-153.4345	360	UAGI	80/10/29	
AUM	Augustine Mound	59.3710	-153.3528	106	UAGI	75/09/00	80/10/29
AUP	Augustine Pinnacle	59.3623	-153.4205	1033	UAGI	88/10/01	
AUW	Augustine West	59.3670	-153.4708	320	UAGI	91/07/27	
BAL	Baldy	61.0353	-142.3472	1265	USGS	73/08/24	
BC3	Beaver Creek U3	63.0658	-141.7827	848			
BCP	Bancas Point	59.9533	-139.6350	396	USGS	79/09/04	
BCS	Bancas Point	59.9483	-139.6167	10	USGS	76/06/25	79/09/04
BGA	Beluga	61.2223	-150.9658	20	USGS	75/10/08	76/03/27
BGM	Big Mountain	59.3927	-155.2293	625	USGS	78/09/08	

BIG	Big Mountain	59.3890	-155.2170	567	USGS	72/07/31	78/09/08
BLR	Black Rapids	63.5017	-145.8450	810	NOAA	65/03/00	85/08/08
BLY	Burwash Landing	61.3725	-139.0260	799	USGS	74/07/22	78/06/01
BMR	Bremner River	60.9682	-144.6030	823	USGS	79/08/19	85/07/16
BRW	Barrow	71.3033	-156.7483	0	UAGI	88/10/01	
CAE	Caetani River	60.0842	-140.9888	716	USGS	83/07/25	84/08/27
CCB	Clear Creek Butte	64.6467	-147.8055	219	UAGI	83/09/16	
CDA	Cape Douglas	58.9553	-153.5295	386	UAGI	78/01/01	81/08/16
CDD	Cape Douglas	58.9298	-153.6430	622	UAGI	81/08/17	
CDL	Candle	66.1140	-161.6567	312	UAGI	78/12/16	
CFI	College Fiord	61.1827	-147.7665	3	USGS	74/07/31	
CGB	Congabuna	61.0690	-151.4525	160	USGS	75/10/08	76/03/27
CGL	Capps Glacier	61.3077	-152.0067	1082	USGS	81/09/22	
CHX	Chaix Hills	60.0630	-141.1167	1067	USGS	74/09/04	85/08/25
CKK	Chekok Lake	59.9597	-154.2332	732	USGS	72/07/29	78/09/09
CNP	China Poot	59.5258	-151.2360	564	USGS	83/07/01	
COL	College Outpost	64.9000	-147.7933	320	USGS	64/01/00	
CRP	Crater Peak	61.2670	-152.1555	1622	USGS	81/08/26	
CRQ	Cirque	60.7567	-143.1392	1853	USGS	88/07/01	
CSG	Childs Glacier	60.6610	-144.8550	678	USGS	84/07/22	85/08/10
CTG	Chitna Glacier	60.9660	-141.3383	1490	USGS	79/08/28	
CUT	Chulitna	62.4047	-150.2695	168	UAGI	86/07/18	
CVA	Cordova	60.5473	-145.7455	120	USGS	71/08/31	
CYT	Cape Yakataga	60.0745	-142.4113	323	USGS	78/08/08	80/09/22
DDM	Donnely Dome	63.7857	-145.8575	900	UAGI	90/08/10	
DFR	Drift River	60.5918	-152.6860	1090	USGS	88/08/15	
DLY	Dezadeash Lake	60.3700	-137.0650	738	GSC		
DMA	Devil Mountain	66.2967	-164.5225	238	UAGI	77/08/00	82/00/00
DMW	Delta Microwave	64.0538	-145.7253	346	UAGI	86/00/ 0	90/08/19
DOT	Dot Lake	63.6487	-144.0625	671	UAGI	88/10/01	
DSB	Disenchantment Bay	60.0767	-139.5450	640	USGS	74/09/08	76/06/08
DSK	Disk Island	60.5020	-147.6468	15	USGS	74/07/27	76/06/07
DWY	Dawson City	64.0533	-139.4317	346	GSC		76/06/07
ERN	Ernestine	61.4442	-145.1123	570	USGS	71/09/16	73/08/29
FBA	College Outpost	64.9000	-147.7933	320	UAGI	91/08/01	
FID	Fidalgo	60.7288	-146.5965	488	USGS	74/10/07	
FIS	Fire Island	61.1442	-150.2185	76	USGS	74/09/24	76/05/04
FYU	Fort Yukon	66.5660	-145.2317	137	UAGI	88/10/01	
GAR	Garner	63.8370	-148.9712	590	UAGI	87/10/20	

GBY	Granite Bay	60.4322	-147.9783	495	USGS	85/07/21	
GHO	Gloryhole	61.7722	-148.9242	1021	USGS	84/09/11	
GIL	Gilmore Creek	64.9750	-147.4950	350	NOAA	67/10/13	
GKC	Gold King Creek	64.1787	-147.9347	490	UAGI	76/07/00	86/03/10
*GLB	Gilahina Butte	61.4418	-143.8105	845	USGS	73/08/25	
GLC	Glacier Island	60.8907	-147.0730	3	USGS	72/07/24	84/09/17
GLI	Glacier Island	60.8797	-147.0942	429	USGS	84/09/17	
GLM	Gilmore Dome	64.9873	-147.3890	820	UAGI	88/10/01	
GLN	Glennallen	62.1108	-145.5488	457	UAGI	86/00/00	
GMA	Granite Mountain	65.4287	-161.2320	858	UAGI	70/09/17	
GYO	Guyot	60.1463	-141.4715	183	USGS	76/06/01	
HAD	Harding Lake	64.4057	-146.9408	427	UAGI	77/09/00	
HIN	Hinchinbrook Island	60.3968	-146.5017	611	USGS	74/10/03	
HMT	Hamilton	60.3365	-144.2607	620	USGS	77/08/16	
HOM	Homer	59.6583	-151.6433	198	UAGI	81/01/01	
HQN	Harlequin	59.4517	-138.8770	372	USGS	74/10/01	
HTP	Hatcher Pass	61.7777	-149.2767	917	UAGI		
HUR	Hurricane	62.9787	-149.6433	496	UAGI	77/02/14	
HYT	Haines Junction	60.8250	-137.5040	1416	GSC	81/07/27	
Ill	Iliamna	60.0802	-152.9595	823	USGS	87/09/15	
ILM	Iliamna	60.1820	-152.8162	550	USGS	71/08/07	87/09/16
ILN	Iliamna	60.1820	-152.8162	550	USGS	71/08/07	72/09/30
IMA	Indian Mountain	66.0685	-153.6787	1380	NOAA	79/12/28	
INK	Inuvik	68.2917	-133.5000	40	GSC	69/02/22	
KAI	Kayak Island	59.9268	-144.4163	311	USGS	82/08/ 3	
KDC	Kodiak	57.7478	-152.4917	13	NOAA	78/09/20	
KEY	Kluane Lake	61.0500	-138.5017	785	GSC	78/08/26	81/07/25
KLU	Klutina	61.4928	-145.9202	1021	USGS	72/07/22	
KMP	Kimball Pass	61.5130	-145.0182	1143	USGS	76/08/01	85/07/19
KNI	Knight Island	60.3487	-147.7360	434	USGS	85/07/21	
KNK	Knik Glacier	61.4125	-148.4557	595	USGS	73/08/11	
KRY	Koidern River	61.9700	-140.4083	686	GSC	78/08/29	81/04/01
KTA	Kotzebue	66.8413	-162.5870	24	UAGI	76/09/08	82/00/00
KTH	Kantishna Hills	63.5532	-150.9210	1172	UAGI	88/10/01	
KTM	Katmai	58.3247	-155.3765	945	USGS	73/07/27	75/08/24
KYK	Kayak Island	59.8683	-144.5232	375	USGS	74/10/02	82/08/02
LOU	Louis Bay	60.4655	-147.6443	490	USGS	85/07/15	
LTI	Latouche Island	60.0405	-147.8542	302	USGS	88/07/01	
LVY	Levy	64.2167	-149.2533	230	UAGI	72/07/ 0	89/09/19

MBC	Mould Bay	76.2417	-119.3600	15	GSC	61/10/18	
MCK	Mckinley Park	63.7323	-148.9350	618	UAGI	64/00/00	
MCN	Mcneil River	59.1010	-154.1998	273	UAGI	76/10/15	81/08/22
MID	Middleton Island	59.4278	-146.3390	37	NOAA	76/05/21	
MLS	Malaspina Glacier	59.7667	-140.1500	30	USGS	74/09/ 4	81/09/05
MMN	Mcneil River	59.1852	-154.3367	442	UAGI	81/08/22	
MRN	Martin River	60.5350	-144.0083	957	USGS	75/08/22	76/03/31
MSE	Moose Creek	61.8383	-148.9672	1318	USGS	84/09/11	85/09/30
MSP	Moose Pass	60.4892	-149.3605	160	USGS	73/08/05	
MTG	Montague Island	59.9118	-147.4970	31	USGS	74/10/03	85/07/15
MTU	Montague Island	59.9878	-147.6503	434	USGS	85/07/21	
NCA	Nelchina	61.9937	-146.8242	741	UAGI	86/07/17	90/06/00
NCT	North Cresent	60.5632	-152.9262	1079	USGS	88/08/14	
NEA	Nenana	64.5772	-149.0772	364	UAGI	81/03/ 5	
NGL	North Gasline	60.8208	-149.9982	122	USGS	74/09/26	76/03/27
NIK	Nikolski	52.9743	-168.8518	207	NOAA	71/05/17	76/03/27
NIN	Ninilchik	60.0112	-151.5355	110	USGS	71/08/28	72/08/24
*NKA	Nikishka	60.7430	-151.2380	100	USGS	71/09/14	
NKI	Nikolski	52.9427	-168.8575	8	NOAA	76/03/27	85/12/26
NNL	Ninilchik	60.0443	-151.2893	381	USGS	72/08/24	
NRA	North River	63.8918	-160.5143	107	UAGI	76/08/00	78/06/08
NTK	Nunitak	59.8777	-139.0352	1050	USGS	74/09/09	76/05/31
OCC	Ocean Cape	59.5425	-139.8602	22	USGS	76/01/01	76/04/24
OPT	Oil Point	59.6527	-153.2297	450	UAGI	88/10/01	
PAX	Paxson	62.9708	-145.4687	1130	UAGI	88/10/01	
PCA	[See Pin]						
PCL	Point Campbell	61.1428	-150.0155	90	USGS	73/09/04	74/09/30
PDB	Pedro Bay	59.7878	-154.1925	305	USGS	78/09/09	
PIN	Pinnacle	60.0967	-140.2567	975	USGS	74/09/05	
PLR	Palmer (Usgs)	61.5922	-149.1308	100	USGS	84/09/20	
PMA	Port Moller	55.9787	-160.4972	315	UAGI	91/08/01	
PME	Palmer East	61.6317	-149.0283	232	NOAA	80/08/19	90/03/01
PMR	Palmer Observatory	61.5922	-149.1308	100	NOAA	67/09/01	
PMS	Arctic Valley	61.2447	-149.5605	716	NOAA	67/05/25	
*PNL	Peninsula	59.6677	-139.3970	585	USGS	74/09/02	
*PRG	Portage	60.8645	-149.0202	55	USGS	72/08/29	
PTR	Potter	61.0575	-149.7292	695	USGS	73/08/12	74/09/15
PWA	Houston	61.6508	-149.8787	137	NOAA	77/07/01	
PWL	Port Wells	60.8593	-148.3348	549	USGS	74/08/03	

RAG	Ragged Mountain	60.3870	-144.6752	739	USGS	84/07/22	
RAI	Raspberry Island	58.0605	-153.1592	520	UAGI	75/10/00	
RDS	Richard D. Siegrist	64.8265	-148.1447	510	UAGI	77/06/12	91/07/18
*RDT	Redoubt	60.5732	-152.4053	930	USGS	71/08/09	90/07/19
RED	Redoubt Volcano	60.4198	-152.7718	1064	UAGI	81/11/10	
RGD	Ragged Mountain	60.2192	-144.5457	610	USGS	74/09/30	77/08/16
RIU	Riou	59.8775	-141.2300	15	USGS	76/08/03	81/09/28
RND	Reindeer	63.4062	-148.8528	991	UAGI	88/10/01	
RON	Remote	62.6912	-150.2035	470	UAGI	71/09/22	74/10/31
SAW	Sawmill	61.8082	-148.3330	740	USGS	73/08/31	
SCF	Sheep Creek Facility	61.9947	-150.0392	67	UAGI	71/09/21	75/10/ 7
SCM	Sheep Mountain	61.8333	-147.3277	1020	UAGI	91/08/01	
SCT	Scotty Lake	62.3192	-150.2972	140	UAGI	71/09/21	75/06/ 0
SDE	Sadie Cove	59.4433	-151.2820	770	USGS	83/07/04	84/06/28
SDG	Sourdough	62.5270	-145.5433	625	UAGI	86/01/00	
SDN	Sand Point	55.3413	-160.4972	23	NOAA	78/10/11	
SGA	Sherman Glacier	60.5340	-145.2070	424	USGS	76/08/16	
SHU	Shuyah Island	58.6280	-152.3488	34	UAGI	74/00/00	90/08/27
SII	Sitkinak Island	56.5600	-154.1820	500	UAGI	75/08/09	
SIT	Sitka	57.0570	-135.3245	19	NOAA	40/00/00	
SIY	Silver City	61.0317	-138.4063	785	GSC	79/12/05	80/03/27
SKD	Sitkalidak Island	57.1642	-153.0803	135	UAGI	70/01/01	
*SKL	Skilak	60.5143	-150.2160	640	USGS	71/09/09	84/07/28
*SKN	Skwentna	61.9803	-151.5297	564	USGS	72/08/08	
SLK	Skilak	60.5123	-150.2210	655	USGS	84/07/29	
SLV	Seldovia	59.4713	-151.5805	91	USGS	72/09/30	85/06/29
SMY	Shemya	52.7308	174.1030	58	NOAA	70/11/17	
SPU	Spurr	61.1817	-152.0543	800	USGS	71/08/10	
SSN	Susitna	61.4638	-150.7433	1297	USGS	72/08/15	
SSP	Sunshine Point	60.2050	-142.8300	305	USGS	74/09/10	
SST	Susitna	61.4342	-150.7803	780	USGS	71/08/24	72/08/ 9
STG	Stephens Glacier	61.4207	-146.3948	1326	USGS	74/07/11	76/01/31
STY	Stony River	61.1445	-154.2018	1047	USGS	72/07/24	75/07/28
SUK	Suckling Hills	60.0737	-143.7770	454	USGS	74/10/02	85/08/10
SVG	Savoonga	63.6950	-170.4800	15	UAGI	77/08/17	
SVW	Sparrevohn	61.1082	-155.6217	762	NOAA	67/08/ 0	
SWD	Seward	60.1037	-149.4493	91	USGS	72/08/22	
TGL	Tana Glacier	60.7558	-142.8297	1234	USGS	88/07/01	
TLK	Talkeetna Mountains	62.4938	-147.8780	1719	USGS	74/07/10	76/07/01

TMW	Tok Microwave	63.3213	-142.9913	488	UAGI	90/08/20	
TNN	Tanana	65.2567	-151.9117	504	UAGI	65/01/00	79/01/03
TOA	Tolsona	62.1048	-146.1723	909	NOAA	71/09/15	
TSI	Tsina	61.2262	-145.3373	1113	USGS	76/08/15	85/07/17
TTA	Tatalina	62.9300	-156.0220	914	NOAA	78/09/20	
TTV	Terentiev Lake	61.0548	-147.1215	533	USGS	84/09/19	85/07/14
TZO	Tzero	63.8027	-145.7350	602	UAGI	87/10/00	89/07/17
*VLZ	Valdez	61.1322	-146.3338	17	USGS	71/09/02	
VZS	Valdez South	61.0442	-146.3053	668	USGS	72/07/22	76/08/15
VZW	Valdez West	61.0590	-146.5540	796	USGS	72/07/17	
WAX	Waxell Ridge	60.4482	-142.8510	991	USGS	75/08/22	
WHC	Whitehorse	60.7367	-135.0983	732	GSC	71/09/01	
WLM	Willow Mountain	61.7737	-145.1980	985	USGS	71/09/01	72/08/00
WRG	White River Glacier	60.0375	-142.0328	550	USGS	74/09/10	
WRH	Wood River Hill	64.4713	-148.0898	314	UAGI	83/09/16	
XLV	Seldovia	59.4547	-151.6717	320	UAGI	91/06/20	
YAH	Yahtse	60.3585	-141.7450	2135	USGS	74/09/05	
YKA	Yellowknife Array	62.4932	-114.6053	200	GSC	62/00/00	
YKC	Yellowknife	62.4783	-114.4733	198	GSC	64/07/15	
YKG	Yakataga	60.0700	-142.4222	46	USGS	72/10/08	85/09/03
YKT	Yakutat	59.4517	-138.8770	372	USGS	72/10/06	74/09/30
YKU	Yakutat	59.5538	-139.7250	40	NOAA	78/09/20	
BRLK	Bradley Lake	59.7638	-150.8897	622	USGS	80/10/11	84/06/30
BRNE	Bradley Lake NE	59.9108	-150.6522	1219	USGS	80/10/12	84/06/28
BRNW	Bradley Lake NW	59.8375	-151.1692	582	USGS	80/10/03	84/06/28
BRSE	Bradley Lake SE	59.7055	-150.6708	975	USGS	80/10/10	87/07/02
BRSW	Bradley Lake SW	59.6410	-151.0448	951	USGS	80/10/12	84/06/28
CBHL	Heather Lake	61.0292	-146.9313	3	USGS	83/07/14	83/09/30
CBKL	Kadin Lake	61.1105	-147.1935	275	USGS	83/07/15	83/09/30
CBLB	Long Bay	60.9655	-147.2217	5	USGS	83/07/15	83/09/30
CBUI	Unakwik Inlet	60.9110	-147.5453	8	USGS	83/09/11	83/09/30
ECNI	Chenega Island	60.2823	-148.0352	4	USGS	87/07/09	87/08/07
EFLB	Foul Bay	60.5823	-148.0608	4	USGS	87/07/09	87/08/07
EGRI	Green Island	60.2922	-147.3895	4	USGS	87/07/09	87/08/07
ELAI	Latouche Island	60.0613	-147.8183	4	USGS	87/07/09	87/08/07
EMTC	Montana Creek	62.1592	-150.0167	131	USGS	86/08/28	86/09/11
ENKI	Naked Island	60.6307	-147.4592	4	USGS	87/07/09	87/08/07
EPKS	Parks Highway	62.2550	-150.2417	99	USGS	86/08/28	86/09/11
ETAL	Talkeetna	62.3042	-150.0820	137	USGS	86/08/28	86/09/11

EWTF	West Fork	62.3188	-150.4758	200	USGS	86/08/28	86/09/11
GALN	Galena Bay	60.9578	-146.7413	3	USGS	72/07/14	72/08/13
JACK	Jack Bay	61.0043	-146.5172	30	USGS	72/07/14	72/08/13
LOWE	Lowe River	61.0695	-146.0428	58	USGS	72/07/14	72/08/13
MNRL	Mineral Creek	61.2100	-146.3193	236	USGS	72/07/14	72/08/13
SENW	Saint Elias NW	60.2300	-140.9067	1250	USGS	79/07/20	79/08/17
SHOU	Shoup Bay	61.1307	-146.5710	15	USGS	72/07/14	72/08/13
SWML	Sawmill Bay	61.0657	-146.7785	15	USGS	72/07/14	72/08/13

Table 2. Alaska Velocity Models

Model 1. Gulf of Alaska

Layer	Depth (km)	P velocity (km/s)
1	0-7	5.0
2	7-12.5	6.8
3	below 12.5	8.1

Model 2. Southern Alaska

Layer	Depth (km)	P velocity (km/s)
1	0-4	5.3
2	4-10	5.6
3	10-15	6.2
4	15-20	6.9
5	20-25	7.4
6	25-33	7.7
7	33-47	7.9
8	47-65	8.1
9	below 65	8.3

Model 3. Northern Alaska

Layer	Depth (km)	P velocity (km/s)
1	0-24.4	5.90
2	24.4-40.2	7.40
3	40.2-76	7.90
4	76-301	8.29
5	301-545	10.40
6	below 545	12.60

Table 3. Geographical regions used to assign starting depth, velocity model, and delay models.

Earthquake Location	Trial Depth (km)	Velocity Model	Delay Model
Gulf of Alaska*	10.	1	2
Southern Alaska (South of 62.5°N)	0., 7.5, 75.	2	1
Northern Alaska (North of 62.5°N)	0., 7.5, 75.	3	1

*(south of a line connecting 56°N, 154°W; 59.5°N, 146°W; 59.7°N, 143°W; 58.2°N, 139°W; 57.9°N, 137.3°W; 56°N, 135°W).

Table 4. P-phase and S-phase traveltime delays

Station	Model 1		Model 2	
	P delay (sec)	S delay (sec)	P delay (sec)	S delay (sec)
HTP	01.10	00.00	00.00	00.00
ILI	00.44	00.78	01.11	01.98
ILM	00.44	00.78	00.44	0.783
ILN	00.44	00.78	00.44	0.783
NIN	01.47	02.59	00.67	01.19
NKA	02.16	03.82	01.45	02.58
NNL	01.47	02.59	00.75	01.34
PWA	00.70	01.25	00.41	0.730
RDT	00.36	00.64	-0.74	-1.32
SKL	00.10	00.18	00.10	0.178
SLK	00.10	00.18	-0.23	-0.41
SPU	00.39	00.69	00.39	0.694
SSN	00.67	01.19	00.30	0.534
SST	00.67	01.19	00.67	01.19
RDTE	00.36	00.64	-0.74	-1.32
RDTN	00.36	00.64	-0.74	-1.32
RDTZ	00.36	00.64	-0.74	-1.32

Table 5. Statistics of available summary/phase data

The total number of sum records is: 53441		
Sum #	type	Description of event type in column 90 of summary record
53,178	Blank, 1, or E	Local or regional tectonic earthquake
18	A	Artillery blast or other explosive device from military base
32	G	Glacial event
5	N	Nuclear blast with hypocenter solution from published catalog
78	Q	Quarry/mine blast
107	R	Regional earthquake with hypocenter solution from published catalog
11	T	Teleseism with hypocenter solution from published catalog
1	X	Volcano X or spindle
11	a	a-type, VT, volcano tectonic

APPENDIX A

Summary of HYPOELLIPSE Data Formats

Data formats are illustrated here for many of the input and output items archived in this report. Each field includes a typical entry, an abbreviated explanation, and the format for reading the field. For more details, refer to the sections indicated in the HYPOELLIPSE manual (Lahr, 1989). Note that the formats listed below for the "Station – time dependent" and "Archive arrival time" records are for the original non-Y2K version of HYPOELLIPSE where only a two-digit year is used and does not include the century.

Station - primary (See section 2.2.5)

1	2	3	4	5	6	7	8	9	1	1	1	1	1	1	1	1	1	2	2	2	2	2	2	2	2	2	3	3	3	3	3	3	3	3	3	4	4	4	4	4	4	4	4	4	4	5	5	5	5	5	5
									0	1	2	3	4	5	6	7	8	9	0	1	2	3	4	5	6	7	8	9	0	1	2	3	4	5	6	7	8	9	0	1	2	3	4	5	6	7	8	9	0	1	2	3	4	5
	B	R	K	6	0	N	2	6	.	2	3		1	4	0	W	2	8	.	2	2			2	4	0		2	2		2	0	0		6	0	0	5				0				0				0				0
St Name				LAT			LAT MIN					LON			LON MIN					ELEV				Mod	T	THK1				THK2				D	PDLY 1				SDLY 1				PDLY 2				SDLY 2			
A4				i2			F5.3					i3			F5.3					i5				i2	I	F4.2				F4.2				A	F4.2				F4.2				F4.2				F4.2			

5	5	5	5	6	6	6	6	6	6	6	6	6	6	7	7	7	7	7	7	7	7	7	8
6	7	8	9	0	1	2	3	4	5	6	7	8	9	0	1	2	3	4	5	6	7	8	9	0
			0				0			2	0			1	0			3	0		-	3	0	Z
PDLY 3				SDLY 3				PDLY 4				SDLY 4				PDLY 5				SDLY 5				C
F4.2				F4.2				F4.2				F4.2				F4.2				F4.2				A

Station - time dependent (See section 2.2.5) Note: in the Y2K version (Lahr, 1999), the expiration date in columns 38-47 has a four-digit year that includes the century and is cnyrmody hr, which is read by (i8, i2).

1	2	3	4	5	6	7	8	9	1	1	1	1	1	1	1	1	1	2	2	2	2	2	2	2	2	2	3	3	3	3	3	3	3	3	3	4	4	4	4	4	4	4	4	4	5	5	5	5	5	5
									0	1	2	3	4	5	6	7	8	9	0	1	2	3	4	5	6	7	8	9	0	1	2	3	4	5	6	7	8	9	0	1	2	3	4	5	6	7	8	9	0	1	2	3	4	5
	B	R	K	*		1				9			4	9			8	0	0					1		0		1	.	0					3	2	8	9	1	2	3	1	2	3	0	2		-	2	7				
St Code				*	ST WT				SYS	5Hz Cal				Xmag C10				XMg Cor		X		F	FMg Cor				P	S		GN		A	YR MO DY				HR MN				Tel Cor				X	X	X	X			
A4				A	F4.2				i2	F4.0				F5.2				F4.2		I		I	F4.1				I	I		i2		I	i6				i4				F4.2				A	A	A	A			

5	5	5	5	6	6	6	6	6	6	6	6	6	6	7	7	7	7	7	7	7	7	8	8	8	8	8	8	8	8	8	9	9	9	9	9	9	9	9	9	1	1	1	1	1	1	1	1	1	1
6	7	8	9	0	1	2	3	4	5	6	7	8	9	0	1	2	3	4	5	6	7	8	9	0	1	2	3	4	5	6	7	8	9	0	1	2	3	4	5	6	7	8	9	0	0	0	0	0	0	0
			0	N	R	+	-	?	?							0			3	3	1	2	.	2	1		1	1			4	1	1	5	.	3	4		1	2			7	8		8	.	7	6		1	3
Alt Cor				P	P	P	P	P	P					SYS	5Hz Cal				Xmag C10					SYS	5Hz Cal				Xmag C10					SYS	5Hz Cal				Xmag C10					SYS							
F4.2				A	A	A	A	A	A					i2	F4.0				F5.2					i2	F4.0				F5.2					i2	F4.0				F5.2					i2							

1	1	1	1	1	1	1	1	1	1	1	1	1	1	1	1	1	1	1	1	1	1	1	1	1
1	1	1	1	1	1	1	1	1	1	2	2	2	2	2	2	2	2	2	3	3	3			
0	1	2	3	4	5	6	7	8	9	0	1	2	3	4	5	6	7	8	9	0	1	2		
	1	5	4		5	.	2	1	2	7	.	2	3	2	9	.	2	2		3	9	0		
5Hz Cal				Xmag C10					Revised Lat					Revised Lon					Rev Elev					
F4.0				F5.2					F5.3					F5.3					i4					

Arrival time (See section 2.2.6.2)

1	2	3	4	5	6	7	8	9	1	1	1	1	1	1	1	1	1	2	2	2	2	2	2	2	2	2	3	3	3	3	3	3	3	3	3	4	4	4	4	4	4	4	4	4	5	5	5	5	5	5
									0	1	2	3	4	5	6	7	8	9	0	1	2	3	4	5	6	7	8	9	0	1	2	3	4	5	6	7	8	9	0	1	2	3	4	5	6	7	8	9	0	1	2	3	4	5
	B	R	K	I	P	U	2		7	9	0	8	0	6	1	0	4	1	1	5	.	3	1								1	9	.	3	8	E	S		3						2	2		1	0					
St Name					M	W		YR MO DY HR MN										SEC.												S-SEC					SRMK		W				Mx AMP				PER								
A4					A2		A	I	I	i10										F5.2										F5.2					A3		I				F4.0				F3.2						

5	5	5	5	6	6	6	6	6	6	6	6	6	6	7	7	7	7	7	7	7	7	7	8	8	8	8	8	8	8	8	8	9	9	9	9	9	9	9	9	9	1	1	1	1	1	1	1	1	1	1
6	7	8	9	0	1	2	3	4	5	6	7	8	9	0	1	2	3	4	5	6	7	8	9	0	1	2	3	4	5	6	7	8	9	0	1	2	3	4	5	6	7	8	9	0	0	0	0	0	0	0	0	0
																																									0	1	2	3	4	5	6	7	8	9
					0	0	T	L					0			2	0	0																											E	E	E	E	E
					S	V	Rmk			Tim Cor				F-P Time																															P	P	S	A	C
					I	I	A2			F5.2				F5.0																															A	A	A	A	A

Instruction (See section 2.2.6.3)

1	2	3	4	5	6	7	8	9	1	1	1	1	1	1	1	1	1	2	2	2	2	2	2	2	2	2	3	3	3	3	3	3	3	3	3	4	4	4	4	4	4	4	4	4	5	5	5	5
									0	1	2	3	4	5	6	7	8	9	0	1	2	3	4	5	6	7	8	9	0	1	2	3	4	5	6	7	8	9	0	1	2	3	4	5	6	7	8	9	0
M	O	R	E					*	E								1	0																				6	1	N	3	1	.	5	2					
IPRO								S	T								S	F	TRIAL Z																								LAT		LAT MIN						
A4								A	A								I	I	F5.2																								F2.0	A	F5.2						

5	5	5	5	5	5	6	6	6	6	6	6	6	6	6	7	7	7	7	7	7	7	7	7	7	8
4	5	6	7	8	9	0	1	2	3	4	5	6	7	8	9	0	1	2	3	4	5	6	7	8	9	0
1	4	2	W	5	9	.	0	1												4	2	4	0	.	1	3
LON				LON MIN				CUSP ID												Min		SECONDS				
F3.0			A	F5.2				A10												F2.0		F5.2				

Archive arrival time (See section 2.2.15) Note: the raw, uncorrected first motion data are provided in column 7 while the first motions corrected for polarity reversals are in column 65. The archived P- and S-phase arrivals times have been corrected for satellite delays. The number of satellite hops (NHOP) in the telemetry path, each producing a delay of 0.27 s is given in column 110. (If the P-arrival and S-arrival sources are not the same, then NHOP is set according to the P-arrival source.) A complete listing of the source codes listed in columns 105-109 which were used for Alaska processing are provided in section 4.2.2.2.

1	2	3	4	5	6	7	8	9	1	1	1	1	1	1	1	1	1	1	2	2	2	2	2	2	2	2	2	2	3	3	3	3	3	3	3	3	3	4	4	4	4	4	4	4	4	4	4	5	5	5	5	5
									0	1	2	3	4	5	6	7	8	9	0	1	2	3	4	5	6	7	8	9	0	1	2	3	4	5	6	7	8	9	0	1	2	3	4	5	6	7	8	9	0	1	2	3	4
	B	R	K	I	P	U	2		7	9	0	8	0	6	1	0	4	1	1	5	.	3	1			6	2		2	9	1	9	.	3	8	E	S		3	1	0	5			2	2		1		2	1	3	8
St Code					M	W	YR MO DY HR MN												Seconds					DIST			AZIM			S-SEC					SRMK	W	A INC			MX Amp				PER			PTT Cal				
A4				A2	A	I	I10												F5.2					F4.1			i3			F5.2					A3	I	i3			F4.0				F3.2			F4.2				

5	5	5	5	5	6	6	6	6	6	6	6	6	6	6	7	7	7	7	7	7	7	7	7	8	8	8	8	8	8	8	8	8	9	9	9	9	9	9	9	9	9	1	1	1	1	1	1	1	1	1	1	1
5	6	7	8	9	0	1	2	3	4	5	6	7	8	9	0	1	2	3	4	5	6	7	8	9	0	1	2	3	4	5	6	7	8	9	0	1	2	3	4	5	6	7	8	9	0	0	0	0	0	0	0	0	0	1
																																										0	1	2	3	4	5	6	7	8	9	0
	9	0	M	S	H	0	0	T	L	D					0			2	0	0			6	2	1	1	3	1					8	2			0			0		2	9		1	1	6	2	3	E	E	E	E	E	1
P SE			R	INS			S	V	Rmk		M	TIM COR					F-P TIME					P RESIDU				S SE		R	S RESIDU						PDLY			SDLY			EDLY			SYS		xmg		fmg		P	P	S	A	C	H
F3.2			A	A2			I	I	A2		A	F5.2					F5.0					F5.2				F3.2		A	F5.2						F3.1			F3.1			F3.1			i2		F2.1		F2.1		A	A	A	A	A	I

Comment Record Codes

C*	Routine comment record in archive arrival times pickfiles
C*(F)	Pickfile id number
C*<C>	Data from Geological Survey of Canada (GSC) Pacific Geoscience Centre (PGC) catalog
C*<I>	Data from International Seismological Centre (ISC) catalog
C*<N>	Data from USGS National Earthquake Information Center (NEIC) catalog

Summary (See section 2.4.1) Note: in the Y2K version, everything is pushed to the right by 2 columns to allow for the century in columns 1-2.

1	2	3	4	5	6	7	8	9	1	1	1	1	1	1	1	1	1	2	2	2	2	2	2	2	2	3	3	3	3	3	3	3	3	3	4	4	4	4	4	4	4	4	4	5	5	5	5	5
									0	1	2	3	4	5	6	7	8	9	0	1	2	3	4	5	6	7	8	9	0	1	2	3	4	5	6	7	8	9	0	1	2	3	4	5	6	7	8	9	0	1	2	3	4
8	9	0	8	0	6	1	0	4	1	0	5	1	0	4	3	N	1	6	3	2	1	2	2	W	4	9	5	3				0	0	4	2		1	5	2	2	0		8	2			4	9		3	1		2

YR MO DY	HR MN	SEC	TLA		LAT Min	LON		LON Min	DEPTH	Mag	N Pha	GAP	Dist 1	RMS	AZIM	Dip
i6	i4	F4.2	i2	A	F4.2	i3	A	F4.2	F5.2	F2.1	i3	i3	F3.0	F4.2	i3	i2

5	5	5	5	5	6	6	6	6	6	6	6	6	6	6	7	7	7	7	7	7	7	7	7	8	8	8	8	8	8	8	8	8	9	9	9	9	9	9	9	9	9	1	1	1	1	1	1	1	1	1	1	1	1	1	1
5	6	7	8	9	0	1	2	3	4	5	6	7	8	9	0	1	2	3	4	5	6	7	8	9	0	1	2	3	4	5	6	7	8	9	0	1	2	3	4	5	6	7	8	9	0	0	0	0	0	0	0	0	0	1	1	1	1	1	1
																																										0	1	2	3	4	5	6	7	8	9	0	1	2	3	4	5
	8	2	2	1	2	1		4		6	3	8	2	0	2	2	F	1	2	5	7	C	F		3	/	M	O	R	E	1	0	7	9	E	0	E	0	1	9	3		7	8	1		5		4		1	7	7		3		-	1	3	2

STD Err	AZIM	Dip	STD Err	xmg	fmg	P	STD Err	Q	M	NS	/	INST	MO YR	T	F	SEQ NUM	S-P TIM	Zup	Zdn	Vp/Vs	WtO	DEPTH
F4.2	i3	i2	F4.2	F2.1	F2.1	A	F4.2	A	A	i2	A	A4	i4	A	I	A5	F4.2	F2.0	F2.0	F4.2	i2	F5.2

Event Type Codes

Event type code in column 90 (A1 format) of non-Y2K HYPOELLIPSE summary record	
A	Artillery blast or other explosive device from military base
a	Volcano tectonic, a-type
E, 1, or blank	Local or regional earthquake
G	Glacial
N	Nuclear blast
Q	Quarry/mine blast
R	Regional earthquake with location from published bulletin
T	Teleseism
X	Emergent, low frequency near volcano

APPENDIX B

List of Previously Published Catalogs

Lahr, J.C., Page, R.A., and Thomas, J.A., 1974, Catalog of earthquakes in south central Alaska, April-June 1972, U.S. Geological Survey Open-File Report, 35 p.

Fogleman, K.A., Stephens, Christopher, Lahr, J.C., Helton, S.M., and Allan, M.A., 1978, Catalog of earthquakes in southern Alaska, October-December 1977, U..S. Geological Survey Open-File Report 78-1097, 28 p.

Stephens, C.D., Lahr, J.C., Fogleman, K.A., Allan, M.A., and Helton, S.M., 1979, Catalog of earthquakes in southern Alaska, January-March 1978, U.S. Geological Survey Open-File Report 79-718, 31 p.

Stephens, C.D., Astrue, M.A., Pelton, J.R., Fogleman, K.A., Page, R.A., Lahr, J.C., Allan, M.A., and Helton, S.M., 1982, Catalog of earthquakes in southern Alaska, April-June 1978, U.S. Geological Survey Open-File Report 82-488, 36 p.

Stephens, C.D., Lahr, J.C., Fogleman, K.A., Helton, S.M., Cancilla, R.S., Tam, Roy and Baldonado, K.A., 1980, Catalog of earthquakes in southern Alaska, October-December 1979, U.S. Geological Survey Open-File Report 80-2002, 53 p.

Stephens, C.D., Fogleman, K.A., Lahr, J.C., Helton, S.M., Cancilla, R.S., Tam, Roy and Freiberg, J.A., 1980, Catalog of earthquakes in southern Alaska, January-March 1980, U.S. Geological Survey Open-File Report 80-1253, 55 p.

Fogleman, K.A., Stephens, C.D., Lahr, J.C., Rogers, J.A., Helton, S.M., Cancilla, R.S., Tam, Roy, Freiberg, J.A., and Melnick, J.P., 1983, Catalog of earthquakes in southern Alaska, July-September 1980, U.S. Geological Survey Open-File Report 83-15, 54 p.

Fogleman, K.A., Stephens, C.D., Lahr, J.C., and Rogers, J.A., 1986, Catalog of earthquakes in southern Alaska for 1984, U.S. Geological Survey Open-File Report 86-99, 106 p.

Fogleman, K.A., Stephens, C.D., and Lahr, J.C., 1988, Catalog of earthquakes in southern Alaska for 1985, U.S. Geological Survey Open-File Report 88-31, 113 p.

APPENDIX C

Summary of Timing Criteria

Routine network processing.

October 1, 1971 - September 31, 1973

Time all shocks with:

A. Cook Inlet (stations west of longitude 150°W):
Minimum S-P time ≤ 25 s **and** recorded at 6 or more stations (clearly recorded at 4 or more of these).

B. Valdez (stations east of 150°W):
1. Minimum S-P time ≤ 20 s **and** clearly recorded at 4 or more stations including 2 of WLM, ERN, VLZ and CVA.

or

2. Minimum S-P time ≤ 10 s **and** clearly recorded at 3 stations including 2 of WLM, ERN, VLZ and CVA.

C. Well recorded regional events that have clipped traces **and** do not come from the Aleutians.

October 1, 1973 - September 31, 1974

Time all earthquakes with:

A. Average F-P time ≥ 30 s. F-P is signal duration (see section on magnitude).

or

B. Average F-P time ≥ 15 s **and** minimum S-P time ≤ 5 s.

October 1, 1974 - January 31, 1975

Time all local events in network with average F-P time ≥ 20 s.

February 1, 1975 - September 31, 1977

Time all shocks with:

A. WEST (stations west of 150°W): Average F-P time ≥ 80 s.

B. CENT (stations between 150°W and 145°W): Average F-P time ≥ 20 s.

C. EAST (stations east of 145°W): All events with 3 clearly recorded P-arrivals **and** 1 S-arrival **or** 4 P-arrivals.

October 1, 1977 - September 31, 1980

Time all shocks within the area 58-64°N and 134-156°W (eastern border moved to 134°W from 136°W) with:

A. WEST: Average F-P time ≥ 80 s.

B. CENT: Average F-P time ≥ 20 s.

C. EAST: All events with 3 clearly recorded P-arrivals **and** 1 S-arrival **or** 4 P-arrivals on SCAN **and/or** EAST films.

October 1, 1980 - June 30, 1981

Time all shocks within the area 58-64°N and 134-156°W with:

A. WEST (West of 145°W): Average F-P time ≥ 30 s (WEST and CENT regions combined)

B. EAST: All events with 3 clearly recorded P-arrivals **and** 1 S-arrival **or** 4 P-arrivals on SCAN **and/or** EAST films.

July 1, 1981 - September 30, 1981

Time all shocks within the area 58-64°N and 134-156°W with:

A. WEST: Average F-P time ≥ 30 s.

B. EAST:

1. All events with 3 clearly recorded P-arrivals **and** 1 S-arrival **or** 4 P-arrivals on SCAN film only.

or

2. If an event has a coda on the SCAN film F-P time ≥ 10 s but does not have 4 P's or 3 P's **and** 1 S, check the EAST film for additional arrivals and time if have 4 P's **or** 3 P's **and** 1 S on SCAN **plus** EAST.

or

3. If at any time less than five stations are operating east of 145°W use both SCAN **plus** EAST films to see if have 4 P-arrivals **or** 3 P-arrivals **and** 1 S-arrival.

December 1, 1980 - May 31, 1989

No rereads on magnitude M < 1.0 events unless solution is unacceptable.

October 1, 1981 - March 31, 1984

Network borders for timing reduced to decrease the number of earthquakes processed per month. Northern border moved from 64°N to 63°N. Less emphasize placed on rereading events between latitude 58-59°N and longitude 134-138°W.

Time all shocks within the area 58-63°N and 134-156°W with:

A. WEST: Average F-P time ≥ 30 s.

B. EAST (same as B for July 1 – September 30, 1981)

.

April 1, 1984 - August 31, 1985

Time all shocks within the area 58-62.5°N (northern border moved from 63.0°N to 62.5°N) and 134-156°W with:

A. WEST: Average F-P time ≥ 30 s.

B. EAST (same as B for July 1 – September 30, 1981)

C. Time any earthquake with S-P time ≤ 2 s on SCAN film station except for AGA whose S-P time must be ≤ 1.75 s.

September 1, 1985 - May 31, 1989

Time all shocks within the area 58-62.5°N and 138-156°W (eastern borders moved from 134°W to 138°W due to major reduction of recordable stations in east) with:

A. WEST: Average F-P time ≥ 30 s.

B. EAST (same as B for July 1 – September 30, 1981)

C. Time any earthquake with S-P time ≤ 2 s on SCAN film station except for AGA whose S-P time must be ≤ 1.75 s.

Special Studies

1. Special study of microearthquakes around Anchorage.
Time all shocks with:

January 1, 1979 - December 31, 1979

A. S-P time ≤ 13.5 s at KNK
and
B. P-arrival at SPU **or** MSP **or** SKL before TOA **and** VZW.

January 1, 1980 - March 31, 1984

A. S-P time ≤ 10 s at PMS
and
B. at least one station other than PMS with a F-P coda above 1 cm pk-to-pk for at least 5 s.

April 1, 1984 - May 31, 1989

A. S-P time ≤ 5 s at PMS **or** SSN
and
B. At least one station other than PMS with a F-P coda above 1 cm pk-to-pk for at least 5 s.

2. Special criterion for reduction in timing of aftershocks of February 28, 1979 St. Elias earthquake.

April 1 - September 30, 1979

A. If CHX is operational **and** YAH **or** PIN is working, do not time shocks where:
1. CHX S-P time < 6 s.
and
2. YAH **or** PIN F-P time < 40 s (changed to 25 s for May - September).
and
3. GYO P-arrival ≤ 4 s before CHX P-arrival.

B. If CHX is not working but GYO is, do not time events where:
1. GYO S-P < 7 s.
and
2. YAH **or** PIN F-P time < 25 s.
and
3. GYO P-arrival is before SSP P-arrival.

C. If CHX **and** GYO are out, do not time events where:
   1. SSP **and** PIN P-arrivals are approximately the same time
   and
   2. SSP **and** PIN S-P time < 10 s.

May 2-19, 1982

Special criterion for large aftershock sequence in St. Elias aftershock zone. Time only aftershocks with a measurable coda seen on SCAN film station **or** if YAH amplitude ≥ 20 mm pk-to-pk. This coda criteria only applied to shocks where YAH, WRG, **and** PIN were first three stations seen on SCAN **and** their S-P intervals were about 7 to 9 s.

April 1, 1984 - September 4, 1985

Do not locate events near Icy Bay with:

A. S-P time ≤ 4 s at AGA (**or** S-P time ≤ 5 s at CHX if AGA out)
   and
B. F-P time at YAH and PIN < 10 s. (**or** F-P time < 8 s at AGA if YAH **and** PIN are dead)

3. Bradley Lake array on southern Kenai Peninsula

November 27, 1980 - January 31, 1981

Time any event with S-P time ≤ 10 s at any Bradley Lake station (BRLK, BRNE, BRNW, BRSE, and BRSW).

February 1, 1981 - September 31, 1981

Time any shock with S-P time ≤ 12 s at any Bradley Lake station.

October 1, 1981 - February 28, 1983

Time any shock with S-P time ≤ 12 s at any Bradley Lake station excluding events that arrive at ILM **or** RDT before SLV, **or** BRNE, **or** BRSW, **or** BRSE.

March 1, 1983 - February 28, 1985

Time any earthquake with S-P time ≤ 6 s at one of the Bradley Lake stations or SLV or SWD.

March 1, 1985 - September 19, 1986

Time all events with S-P time ≤ 3.5 s at BRLK.

4. Cook Inlet volcanoes

July 1, 1981 - May 31, 1989

Time any earthquake with S-P time ≤ 5 s at SPU, RDT, **or** ILM on SCAN film.

5. Aftershocks of August 14, 1984, Sutton m_b 5.7 event

September 11, 1984 - April 30, 1986

Time all earthquakes with GHO S-P time ≤ 4 s **and** KNK F-P time ≥ 8 s on SCAN film.

6. Knight Island in Prince William Sound

July 7, 1985 - August 31, 1985

Timed all earthquakes which:

A. Have O wt. P arrivals on KNI, LOU, GBY
   and
B. KNI P-arrival is before GLI **and** MTU P-arrivals
   and
C. GBY S-P ≤ 8 s.
   and
D. A measurable coda on KNI **or** LOU **or** GBY **or** pk-to-pk amplitude ≥ 10 mm on all three stations (KNI, LOU, GBY).

September 1, 1985 - December 31, 1987

Time all shocks with KNI S-P ≤ 7 s **and** F-P ≥ 8 s.

7. Montague Island in southern Prince William Sound

September 1, 1985 - April 30, 1986

Time all events with MTU S-P ≤ 5 s.

8. Joint USGS/GIUA data set

July 1, 1988 - May 31, 1989

Starting in July 1988, the Geophysical Institute of the University of Alaska (GIUA), Fairbanks began recording 13 USGS stations along with their own network. The GIUA locates all events triggered on by their automatic detection and recording system regardless of magnitude or location. Consequently, the GIUA locates shocks within the USGS routine processing borders that would normally not be processed by the USGS. Duplicate readings from USGS stations taken by GIUA staff for earthquakes also processed by the USGS were often weighted out.

9. Merging of data from published bulletins

Data from the National Earthquake Information Center (NEIC), the International Seismological Centre (ISC), and/or the Pacific Geoscience Center (PGC) were added to this catalog during select time periods to improve hypocenter solutions, to facilitate reviews of the seismicity and to improve the magnitude threshold for completeness.